

~~CONFIDENTIAL~~

Copy 6
RM E56D27

NACA RM E56D27

UNCLASSIFIED



RESEARCH MEMORANDUM

PERFORMANCE CHARACTERISTICS OF AN AXIAL-FLOW
TRANSONIC COMPRESSOR OPERATING UP TO TIP
RELATIVE INLET MACH NUMBER OF 1.34

By John W. R. Creagh

Lewis Flight Propulsion Laboratory
Cleveland, Ohio

CLASSIFICATION CHANGED
UNCLASSIFIED

Copy of T.P.A. # 27 Date 7-28-60 GA

CLASSIFIED DOCUMENT

This material contains information affecting the National Defense of the United States within the meaning of the espionage laws, Title 18, U.S.C., Secs. 793 and 794, the transmission or revelation of which in any manner to an unauthorized person is prohibited by law.

NATIONAL ADVISORY COMMITTEE
FOR AERONAUTICS

WASHINGTON

August 17, 1956

~~CONFIDENTIAL~~ UNCLASSIFIED



3 1176 01435 8502

UNCLASSIFIED

NACA RM E56D27

NATIONAL ADVISORY COMMITTEE FOR AERONAUTICS

RESEARCH MEMORANDUM

PERFORMANCE CHARACTERISTICS OF AN AXIAL-FLOW TRANSONIC COMPRESSOR

OPERATING UP TO TIP RELATIVE INLET MACH NUMBER OF 1.34

By John W. R. Creagh

SUMMARY

Performance characteristics of an axial-flow transonic-compressor rotor were investigated over a range of inlet relative Mach numbers up to 1.34. Design tip speed of the compressor was 1300 feet per second; inlet hub-tip radius ratio, 0.50; and design specific weight flow, 31.1 pounds per second per square foot of rotor frontal area. The blades had double-circular-arc profiles. Over-all blade-element and radial variations of pertinent flow parameters are presented for a range of weight flow at equivalent tip speeds of 975, 1100, 1200, and 1300 feet per second.

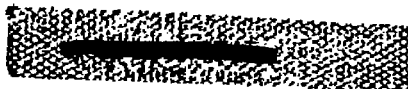
The compressor choked at a corrected weight flow slightly less than the design value. The relative total-pressure-loss coefficients obtained for design-speed operation were considerably greater than those assumed in the design; the resultant increase in discharge axial velocity level caused significant reduction in work input and adiabatic efficiency. Considerations of hub choking indicate that isentropic flow equations are inadequate for determining design incidence angles in this region. The simple-radial-equilibrium concept was reasonably accurate in determining the axial velocity distribution behind the rotor except near the hub, where the radial-flow term of the complete equilibrium equation could not be neglected. The data of this report extend previously reported correlations of incidence- and deviation-angle corrections and a total-pressure-loss parameter to higher Mach numbers. No significant changes to these correlations were noted, but some evidence was found to indicate that the blade suction-surface Mach number may be a parameter in the plots of total-pressure-loss parameter against diffusion factor.

INTRODUCTION

The advantages of operating axial-flow compressors in the transonic range are experimentally demonstrated in references 1 and 2 up to

UNCLASSIFIED

UNCLASSIFIED



T000

CU-1

tip relative inlet Mach numbers of 1.10. As a result of the improvements in performance obtained in that investigation, an extensive research program was initiated to obtain more complete information on the operating characteristics of compressors in the transonic range of inlet relative Mach number. Emphasis has been placed on determining the performance of the double-circular-arc airfoil at these Mach numbers both because it was analytically determined in reference 3 that this airfoil is a suitable shape for operation at a Mach number in the vicinity of 1.20 and because of the background of information on this blade shape in subsonic cascades (e.g., refs. 4 and 5). Because two-dimensional-cascade tests have not always been completely adequate in describing compressor flow conditions, particularly in regions of the compressor where three-dimensional-flow effects predominate (ref. 6), and because of the difficulty of obtaining cascade data in the transonic Mach number range, it becomes necessary, or at least expedient, to use rotor tests for this purpose. It is evident that good design control of transonic compressors cannot exist until adequate information is available on their performance in the range of Mach numbers in which they are intended to operate.

Recent investigations of the performance of transonic compressors with double-circular-arc airfoils have determined some of the effects of reducing chord length (ref. 7) and hub-tip radius ratio (ref. 8). In reference 9, the rotor tip inlet relative Mach number range for double-circular-arc blades was extended up to 1.22. In each of these investigations the hub-tip radius ratios, blade aspect ratios, and solidities were characteristic of the front stages of multistage compressors. In reference 10, satisfactory performance was obtained at tip inlet relative Mach numbers up to 1.35 for a rotor with high hub-tip radius ratio, low aspect ratio, and high solidity. The blade shape used on the rotor of reference 10 was analytically derived from a consideration of the principles of reference 11 and was similar to the blade shape recommended in reference 3 for an inlet relative Mach number level of 1.40. This blade shape did not have a double-circular-arc thickness distribution, although, as stated in reference 10, the maximum-thickness position was at approximately the midchord position.

It was considered of interest, therefore, to extend the range of investigation of the double-circular-arc compressor blade profile to a Mach number and tip-speed level somewhat in excess of any previously conducted on this airfoil shape. Since this investigation was an exploratory one, aimed at accumulating blade-element data, conservative values of blade loading were employed in the design and no attempt was made to obtain the maximum performance potential. The desirable features of low hub-tip radius ratio, short chord length, and moderate solidity level, corresponding to large air-flow capacity and light weight, were also incorporated into the compressor design.

The purpose of the present investigation, then, was to obtain information on the performance of a compressor at high inlet relative Mach numbers and tip speeds and at the same time broaden the scope of information on the double-circular-arc airfoil in a rotating cascade. The over-all and blade-element characteristics of the compressor, together with radial variations of rotor-inlet and -outlet parameters, are presented over a range of corrected tip speeds from 975 to 1300 feet per second. Information concerning mass-flow shift and radial pressure equilibrium at the compressor outlet is also included, along with a discussion of some of the problems associated with the satisfactory design of compressors of this type.

COMPRESSOR DESIGN

Velocity-Diagram Calculations

The design of the compressor rotor used in this investigation was initiated by arbitrarily specifying the following:

- (1) Inlet tip diameter of 16 inches
- (2) Inlet tip speed of 1300 feet per second
- (3) Absolute inlet axial Mach number at mean radius of 0.625 and no inlet guide vanes
- (4) Hub-tip radius ratio at inlet of 0.50
- (5) Blade-chord length of 1.75 inches, and tip solidity level of approximately 1.0
- (6) Rotor-inlet and -outlet blockage factors (ref. 2) of 0.98 and 0.96, respectively

With these conditions established and with a tentative limiting value of tip diffusion factor (ref. 12) of 0.40 as a guide, preliminary estimates of the outlet annular area were obtained by assuming a radially constant pressure ratio of 1.60 and several values of both over-all efficiency and inlet-to-outlet axial velocity ratio. The efficiency values were taken as constant along the blade span; this facilitated the computation, since, from the equilibrium equation described in reference 9 (eq. (9)), the discharge axial velocity would then be constant radially. The results of these calculations indicated that, for constant inlet and outlet tip diameters, the hub cone angle was so large that radial velocity components would have assumed obvious importance, a complication considered undesirable for the present investigation. The outlet hub cone angle was therefore reduced sufficiently to produce an outlet

4001

CU-1 back

hub diameter with which a more conventional type of hub shape could be obtained. A satisfactory value of outlet hub diameter was obtained by setting the tip diameter at 15.5 inches; and the resulting hub-tip diameter ratio $r_{h,4}/r_{t,4}$ at the outlet was 0.593. (All symbols are defined in appendix A.) The exact contour of the annulus walls in the vicinity of the rotor was then obtained by fairing curves between the inlet and outlet radii at both the hub and tip. A subsequent calculation was made, assuming a pressure ratio of 1.60 and an efficiency of 0.90, both constant radially, using this annulus-area ratio; and the resultant tip diffusion factor was found to be 0.41. This was believed to be an acceptable value and permitted the continuation of the velocity-diagram computations for the condition of varying efficiency along the blade span.

In order to obtain more realistic values of outlet velocities and blade loading, a radial variation of efficiency was introduced. Values of blade-element losses obtained from several recent investigations of single-stage transonic compressors were studied, with the greatest emphasis arbitrarily placed on the data of reference 7. With the aid of equations developed in reference 2, the selected values of blade-element loss coefficient were converted into a radial variation of efficiency using an energy level corresponding to a radially constant pressure ratio of 1.60 and an efficiency of 0.90. The necessary values of relative inlet Mach number were determined from the preset value of inlet axial Mach number at the mean radius of 0.625 and a radial variation of inlet axial Mach number obtained from an unpublished investigation on the same inlet annulus configuration. The resultant values of blade-element efficiency are shown in table I for several radial stations.

The computations of the outlet velocity triangles were then initiated by assuming a radially constant pressure ratio of 1.60, which, together with the efficiency variation, completely described the radial variation of total pressure, total temperature, and absolute tangential velocity. The static pressure and axial velocity were determined by assuming a trial value of outlet axial velocity at the mean radius. The following equations were used in evaluating the outlet flow parameters:

$$\frac{p_4}{p_{a,4}} = \left(1 - \frac{v_{\theta,4}^2 + v_{z,4}^2}{2gJc_p T_4} \right)^{\frac{1}{\gamma-1}} \quad (1)$$

$$\frac{p_4}{P_4} = \left(\frac{p_4}{p_{a,4}} \right)^{\gamma} \quad (2)$$

$$dp_4 = \frac{\rho_4 V_{\theta,4}^2}{gr_4} dr_4 \quad (3)$$

Equations (1) and (2) established a level of static pressure at the mean radius; and equation (3) was used to establish the radial gradient of pressure usually called simple radial equilibrium, which was assumed applicable in this investigation. From these equations, a complete description of outlet velocity triangles at all radii could be determined for the originally assumed axial velocity. A further requirement, however, was that the equation of continuity be satisfied, or

$$2\pi K_{bk,4} \int_{r_{4,h}}^{r_{4,t}} \rho_4 V_{z,4} r_4 dr_4 = 2\pi K_{bk,3} \int_{r_{3,h}}^{r_{3,t}} \rho_3 V_{z,3} r_3 dr_3 \quad (4)$$

The condition of continuity was satisfied by assuming different values of mean-radius outlet axial velocity and carrying out the computational procedure until agreement between both sides of equation (4) was obtained to within 0.5 percent, which was considered adequate.

For the assumed values of pressure ratio and efficiency, the tip diffusion factor was somewhat high. By specifying a linear variation in pressure ratio from 1.60 at the tip to 1.52 at the hub, the level of diffusion factor was reduced along the blade from hub to tip to a value considered acceptable, and this design condition was chosen as the final one. The design relative inlet Mach number at the tip of the blade was 1.366. The design data are summarized in table I.

Blade Selection and Fabrication

Double-circular-arc blade sections were chosen for each of several selected conical surfaces along the blade span. The mean-line camber angles ϕ were determined from the air-turning angles $\Delta\beta'$ obtained in the velocity-diagram computations, deviation angles δ^0 computed from the empirical design rule of reference 13, and incidence angles i arrived at after a study of available rotor blade-element performance data. [In a recent publication (ref. 6), rules for the estimation of minimum-loss values of incidence and deviation angles are developed from a study of a large amount of data from single-stage-compressor rotor investigations.] Figure 1 shows a typical rotor blade section together with the blade-angle notation used in this report. Table I shows the incidence and deviation angles used in the design. With a prescribed blade chord of 1.75 inches and a general level of solidity of 1.0 at the tip, it was decided to use 27 blades, which resulted in an actual tip solidity of 0.95 based on the average of the inlet and outlet tip radii.

The blade thickness was set at 5 percent of chord length at the tip and 9 percent of chord length at the hub, with hyperbolic variation along the blade span. Isentropic channel flow computations carried out for the hub-section blade element indicated that choking should not occur in this region for the design incidence angle. The leading- and trailing-edge radii were set at 0.010 inch across the entire blade span except near the hub, where, from stress considerations, a fillet of 0.25 inch was used in fairing the blade into the mounting base.

The complete blade shape was specified by radially stacking the several circular-arc sections on their centers of gravity in the assumed streamline planes. Coordinates for blade fabrication were obtained by a graphical projection of the blade shapes from the streamline plane onto planes of constant inlet and outlet radius. After the blades had been constructed, examination of the profiles along several of the design stream surfaces indicated differences in camber angle and blade shape near the tip as compared with the design values. Owing to the presence of an excessive amount of metal on the suction surface near the trailing edge of the blade, the effective camber angle was increased above the design value. Deviation from the double-circular-arc profile was confined to the rearward 25 percent of chord and to the outer 30 percent of the blade span. The inlet and outlet blade angles as designed and as constructed are compared in figure 2. Analysis of the compressor performance was based on the angles obtained from measurements on the blade. The measured coordinates of the tip section of a representative blade are shown in table II along the design stream surface. Figure 3 is a photograph of the rotor and blade assembly.

4001

APPARATUS, INSTRUMENTATION, AND PROCEDURE

Compressor Installation

The experimental rotor of this investigation was installed in a variable-component test rig. Power for driving the compressor was supplied by a 6000-horsepower variable-speed electric motor in conjunction with a speed increaser. Room air, used throughout the investigation, was drawn through an inlet throttle into a large tank (7.5-ft diam. and 15 ft long) installed upstream of the compressor. The air entered the compressor through a smooth bellmouth and was discharged through a collector-mounted throttle and a submerged orifice in the downstream piping into the laboratory exhaust system. A schematic diagram of the test section is shown in figure 4.

Instrumentation

A standard A.S.M.E. submerged-orifice installation (ref. 14) was used to measure the air flow through the compressor.

The location of the instrumentation stations on the compressor test section is shown in figure 4. The inlet tank (station 1) was supplied with standard instrumentation (ref. 15) for measuring pressures and temperatures. At stations 2, 3, and 4, four static-pressure taps were located on both the inner and outer walls at approximately equal circumferential spacing. At station 2, 1.25 inches ahead of the rotor, the static-pressure profile of the airstream was measured by a five-position L-static type rake in conjunction with the wall taps. The tubes on the rake were positioned to be in the centers of equal annular areas and were directed parallel to assumed streamlines in the contracting inlet passage. A correction to the static-pressure readings at station 2 was applied to determine the static-pressure profile at station 3 (0.25 in. ahead of the rotor) by adjusting the level of the profile at station 2 to the static pressures measured at the walls at station 3. The resultant profiles at station 3 were used throughout this investigation in computing the flow parameters at the compressor inlet.

A few radial surveys of total pressure and flow angle entering the rotor were made at station 3 for several weight flows at design speed. These subsidiary tests showed that the entering air contained no tangential velocity and that the difference in free-stream total pressure between stations 1 and 3 was negligible. To determine the total-pressure profile near the inner and outer walls at station 2, a five-position rake was installed at both walls. The tubes on these rakes were 0.050 inch in diameter and were spaced 0.10 inch apart. The tube nearest the wall was set at 0.05 inch from the wall.

Rotor-outlet radial surveys of total pressure, total temperature, absolute flow angle, and static pressure were conducted at station 4, which was 0.25 inch downstream of the rotor disk. Total pressure, total temperature, and flow angle were measured by each of three combination probes (ref. 15) spaced circumferentially. Each of these probes contained two spike-type thermocouple junctions, a total-pressure tube, and a claw-type tube configuration to measure the flow angle. The two thermocouples were connected in series to obtain improvement in the accuracy of reading small temperature rise across the rotor. Static-pressure surveys were conducted with two L-head Prandtl tubes, each having two static-pressure orifices manifolded together. Angle-sensing tubes were mounted on the probe to align it with the airstream. The values of total temperature, total pressure, flow angle, and static pressure used in calculating the performance characteristics of the compressor at each radius were the arithmetic averages of the corresponding readings obtained from each probe.

The static-pressure and temperature-measuring probes were calibrated in an open-jet tunnel for applicable corrections to the experimental readings. The calibration covered the range of Mach numbers encountered

in this compressor investigation. A more complete description of the instrumentation types used, along with photographs, is included in reference 16.

A magnetic pickup mounted in the compressor casing near the rotor blade trailing edge was used to obtain a rough measurement of the magnitude of blade vibration.

Procedure

The investigation of rotor performance was conducted at corrected tip speeds $U_{t,3}/\sqrt{\theta}$ of 1300, 1200, 1100, and 975 feet per second. For each value of tip speed, the weight flow of air was varied from open throttle to a value slightly higher than that which produced unstable pressure and temperature readings. At this unstable point of operation it was noted that the blade tip vibrations were approximately three to four times the normal amplitude for the particular speed. At each value of weight flow, surveys were conducted at the rotor outlet (station 4) to obtain the values of the significant flow parameters at 11 radial positions. Six of these radial positions were selected arbitrarily at 11, 17.5, 33.5, 50, 67, and 83 percent of the annulus passage height from the casing for the purpose of determining blade-element performance data. A complete description of the equations and methods used in obtaining blade-element performance parameters is presented in reference 2.

Throughout the test program the inlet total pressure was maintained at 25 inches of mercury absolute and the inlet total temperature varied from 70° to 80° F. The rotor speed was held to within 0.5 percent of the prescribed value for all the test points. Rotor over-all mass-averaged temperature-rise and momentum efficiencies were obtained by means of equations given in reference 9, and the mass-averaged pressure ratio was obtained from the following equation:

$$\left(\frac{P_4}{P_1}\right)_{\text{m.a.}} = \frac{\int_{r_{4,h}}^{r_{4,t}} \rho_4 V_{z,4} r_4 \left(\frac{P_4}{P_1}\right) dr_4}{\int_{r_{4,h}}^{r_{4,t}} \rho_4 V_{z,4} r_4 dr_4} \quad (5)$$

Reliability of Data

One method used to obtain an estimate of the degree of accuracy of the data in an investigation of this type is to compare the values of

weight flow of air measured by the orifice and by the instrumentation ahead of and behind the compressor rotor. It was found that the values of weight flow measured at the rotor inlet (station 3) agreed with the orifice values within an average of about 1.0 percent, with a maximum error of 1.7 percent, except for the data at a corrected tip speed of 975 feet per second. At that speed the average difference was about 2.0 percent, with an attendant maximum error of 2.5 percent. The rotor-outlet surveys (station 4) indicated agreement with the orifice weight flow within an average of 3.0 percent, with a maximum difference of 4.2 percent. The weight flows measured at the two survey stations were usually lower than the orifice values, and the average percentage differences mentioned therefore represent a decrement in weight flow. In plotting the data of this report, the weight-flow values used for the curves are those obtained from the instrumentation ahead of the rotor (stations 1, 2, and 3).

Another check on the accuracy of the data can be obtained by comparing the mass-averaged adiabatic efficiencies as determined from the temperature rise across the rotor and from the change in the product of angular momentum and rotor angular velocity. The temperature-rise- and momentum-efficiency values agreed within 3 to 4 percentage points over the entire range of weight flow at corrected tip speeds of 1100, 1200, and 1300 feet per second, except for the lowest pressure-ratio points at the two lower speeds. At a corrected tip speed of 975 feet per second, agreement of the efficiencies within these limits was obtained only at the three highest pressure-ratio points. Examination of the data revealed that, where the discrepancy between the efficiencies was greater than 3 to 4 percentage points, the difference could be accounted for either by an error in absolute outlet-air angle of 1.5° to 2.5° or by an error in temperature of 3° to 4° F. Exactly which of these two types of error was predominant could not be determined, but observation of the data indicated that the temperature readings from the three probes were generally much more consistent than the angle readings.

If the largest efficiency differences were to be attributed to errors in angle measurements, it was found that on the average across the radius the deviation angles for the lowest pressure-ratio points at corrected tip speeds of 975, 1100, and 1200 feet per second would be reduced by 0.80° , 0.60° , and 0.50° , respectively. The diffusion factors for these same points would be increased by about 25, 20, and 15 percent, respectively. The corrections for both the deviation angle and the diffusion factor were greater in the hub region than in the tip region. At a corrected tip speed of 975 feet per second the correction in deviation angle and diffusion factor decreased as the pressure ratio increased. At the mid over-all total-pressure-ratio point at this speed, the correction amounted to a reduction in the deviation angle of 0.40° and an increase in the diffusion factor of 10 percent.

It may be concluded that, except for the lowest pressure-ratio points at corrected tip speeds of 1100 and 1200 feet per second and the lower half of the weight-flow range at a corrected tip speed of 975 feet per second, the accuracy of the values of measured total pressure, total temperature, static pressure, and absolute flow angle at the rotor outlet is good. In addition, satisfactory accuracy was believed to have been obtained over the entire weight-flow range at design speed. As to the rest of the data, the values of all parameters that are dependent on the absolute outlet flow angle should be accepted with some reservation.

RESULTS

Over-All Performance

The over-all performance of the compressor is shown in figure 5 for corrected compressor tip speeds of 975, 1100, 1200, and 1300 feet per second over a range of corrected specific weight flows. (As used herein, compressor tip speed refers to the rotor tip speed at the compressor inlet.) The design-point values of corrected weight flow, total-pressure ratio, and efficiency are also included. The experimental values of total-pressure ratio and efficiency shown in figure 5 are mass-averaged values obtained from the surveys at station 4. The letters A, B, C on each of the curves are used in subsequent figures for identification purposes.

At design speed, the maximum pressure ratio obtained was 1.55 and was accompanied by an over-all efficiency of 0.79. At a maximum efficiency for design-speed operation of approximately 0.82, the over-all pressure ratio was 1.51 and occurred at a corrected specific weight flow of 29.2 pounds per second per square foot of frontal area. This point represented a drop in efficiency from the design value of approximately 11 percentage points, a pressure ratio that was about 96 percent of the design value, and a corrected specific weight flow of about 94 percent of the design value. The maximum specific weight flow at design speed was about 98 percent of the design value but was obtained with the compressor operating in a choked condition. Figure 5 shows that the compressor choked prematurely, which prevented it from obtaining design flow at or reasonably near design pressure ratio.

At corrected tip speeds of 1200, 1100, and 975 feet per second, the peak-efficiency values obtained were approximately 0.86, 0.88, and 0.91, respectively, and the corresponding total-pressure ratios were 1.40, 1.35, and 1.24, respectively. The design value of efficiency was not achieved at any of the rotor speeds tested.

Radial Variations of Flow Parameters

Inlet conditions. - Figure 6 shows the variation in inlet absolute Mach number, inlet relative Mach number, and inlet relative air angle with radius for three operating conditions at design speed. Included on the plots are the respective design variations of the pertinent parameters. In general, at the higher weight flows (points A and B, fig. 6(a)) the variation of inlet axial Mach number across the passage was approximately similar to the design variation, but the level of the experimental values was less than that of the design value. As the weight flow decreased, the velocity variation across the passage became negligible except in the vicinity of the hub, where the inner-wall curvature ahead of the rotor resulted in a reduction in axial velocity.

The variations of inlet relative Mach number and inlet relative flow angle across the annulus reflect the lower than design absolute Mach numbers obtained experimentally. Figure 6(c) shows that, except in the vicinity of the tip region, the experimental incidence angles (difference between relative inlet-air angle $\beta_{\frac{1}{2}}$ and measured blade-inlet angle α_3) were greater than the design values. A maximum tip relative inlet Mach number of about 1.34 was obtained at the highest weight-flow point. As shown in figure 6(b), supersonic Mach numbers were obtained over approximately 60 percent of the rotor blade height at the maximum weight-flow point.

Over the range of corrected weight flows at design speed, the blockage factor $K_{bk,2}$ (ref. 2) at the inlet was found to be constant at a value of 0.98. This value was also obtained at the peak-efficiency point at all the other corrected rotor tip speeds. Since this was the value used in the design, the inability of the compressor to obtain the design weight flow at a reasonable pressure ratio cannot be attributed to an increase in the boundary-layer thickness in the inlet annulus.

Outlet conditions. - The variations with outlet radius of total-pressure ratio, adiabatic efficiency, absolute and relative outlet Mach number, absolute outlet-air angle, relative turning angle, and relative total-pressure-loss coefficient are shown in figure 7 for corrected rotor tip speeds of 1300, 1200, 1100, and 975 feet per second. Included in figure 7(a) are the design variations of the various parameters. In general, in the good-efficiency range of operation (point B, fig. 7(a)), the highest pressure-ratio values were obtained in the tip region, which was in accordance with the design specifications of a linear decrease in pressure ratio from tip to hub. Figure 7(a) also illustrates a peculiar radial pressure-ratio variation in the mean-radius region, where a noticeable bump occurred in the curves. This condition did not appear at the lower corrected tip speeds, and the reason for its presence is not understood. Closely spaced surveys in the region of the bump

4001

CU-2 back

indicated a gradual increase to the peak value and then a gradual decrease, as depicted by the curves of figure 7(a). The corresponding relative-turning-angle curves of figure 7(a) show an increase in the mean-radius region, particularly as the corrected weight flow was reduced. Visograph enlargements of blade sections near this pressure-ratio bump were taken from one of the rotor blades, but no definite indication of a local increase in camber angle was observed.

The efficiency curves of figure 7(a) show that the design values chosen were considerably optimistic, especially in the tip region where the experimental values at design speed were 15 to 20 percentage points lower than anticipated. Much better agreement was obtained near the hub region at design speed; and, as the corrected tip speed was reduced, the good-efficiency range moved continuously outward toward the tip.

The radial distribution of absolute Mach numbers at design-speed and peak-efficiency operation was essentially equivalent to the design distribution. The outlet absolute Mach numbers were quite conservative for this operating point, a peak value of 0.70 being obtained near the hub.

At the lower weight flows at design speed, an increase in absolute outlet-air angle can be noted near the blade tip. Examination of the data reveals that in this region of the blade the variation of outlet static pressure with radius was slight. It follows that, since the relative total-pressure-loss coefficient increased rapidly near the blade tip, the relative velocity must have decreased. Subsequent plots show that the deviation angle did not vary appreciably with radius and weight flow in this section of the blade (relative discharge angle was nearly constant); and, therefore, from velocity-diagram considerations, the outlet axial velocity was reduced. This local reduction in axial velocity was responsible for the increase in absolute flow angle near the blade tip. A similar situation existed in the boundary-layer region near the hub, but the effect on the absolute flow angle was not so pronounced. No great deviation from the design absolute-flow-angle variation was obtained for operation at peak efficiency at design speed.

The relative outlet Mach number at choked flow at design speed was considerably greater than the design value and in the tip region was slightly greater than 1.00. The high relative Mach numbers in this region of the blade persisted over the entire speed range for the choked-flow condition and even at the lowest speed tested were about 0.95.

The relative-turning-angle curves demonstrate that, at choked flow at design speed, approximately design turning was obtained over most of the blade span, with some underturning occurring in the vicinity of the hub. Reductions in weight flow with attendant increase in incidence

angle generally resulted in increased turning angle except in the tip region, where an increase in deviation angle at the lower weight flows tended to reduce the turning angle.

The curves of relative total-pressure-loss coefficient show a generally low level outside the boundary layer adjacent to the hub section. A marked increase in loss occurred between the mean and tip blade sections, the largest increase occurring at the highest pressure-ratio point, where the blade loading was the greatest. In this region of the blade the considerable discrepancy between the design and experimental loss-coefficient values is readily observable.

The blockage-factor values obtained from measurements at the rotor discharge showed a slight variation with weight flow at design speed. For the corrected-weight-flow values corresponding to points A, B, and C at this speed (fig. 5), blockage factors of 0.96, 0.95, and 0.945, respectively, were obtained. At weight flows corresponding to points B at the lower speeds, the blockage factor varied between 0.955 and 0.96. In general, then, the design value of outlet blockage factor (0.96) was closely approximated by the experimental data.

Weight-flow distribution. - The radial distribution of weight flow at the inlet and outlet of the compressor is shown in figure 8 for three values of corrected specific weight flow at design speed. The abscissa and ordinate were chosen to make the comparison of weight-flow variations at the two axial stations more discernible by eliminating the difference in the annulus height. From the conventional form of the continuity equation for annular flow,

$$w = 2\pi \int_{r_h}^{r_t} \rho V_z r \, dr \frac{1}{144} \quad (6)$$

If percent of passage height x is defined as

$$x = \frac{r - r_h}{r_t - r_h}$$

then

$$dr = (r_t - r_h) \, dx$$

and equation (6) may be rewritten in the form

$$w = 2\pi \int_{x_h}^{x_t} \rho V_z r (r_t - r_h) \, dx \frac{1}{144} \quad (7)$$

which is the form of the continuity equation expressed in figure 8.

The weight-flow distributions at the compressor-inlet station were quite uniform and did not depart from this uniformity with changes in weight flow or speed. At the highest corrected specific weight flow obtained (30.64, fig. 8), the outlet-station curves show some weight-flow shift from the tip region toward the hub. The magnitude of this radial shift increased as the weight flow decreased; and, at the lowest weight flow at design speed (27.34), a noticeable decrease in weight flow occurred over about 15 percent of the passage height near the tip. Examination of similar weight-flow-distribution plots at peak-efficiency operation (points B, fig. 5) for the lower speeds shows that the radial shift in flow became progressively smaller as the speed decreased. Specifically, the shift in flow demonstrated by the high-weight-flow point at design speed (30.64, fig. 8) was greater than any obtained for operation at the peak-efficiency point at the lower speeds.

Blade-Element Characteristics

The data of this report are presented at six radial stations at both inlet and outlet, conforming to the positions of six streamlines assumed to occur along straight lines joining the same percentage of the annular height at each station. Incidence angle was used as the independent variable and was computed from the measured blade angle and the relative inlet air-flow angle. The blade elements chosen were at 11, 17.5, 33.5, 50, 67, and 83 percent of the annulus height at both the inlet and outlet of the rotor. The several blade elements are hereinafter referred to by their respective percentage values, the smaller numbers (e.g., 11) corresponding to streamlines near the tip and progressing to the larger numbers near the hub. Figure 9 shows the variation with incidence angle of relative total-pressure-loss coefficient, relative inlet Mach number, axial velocity ratio, adiabatic efficiency, deviation angle, diffusion factor, static-pressure-recovery ratio, and a dimensionless work coefficient over the range of corrected weight flows obtained at each of the several corrected rotor tip speeds.

The curves of loss coefficient against incidence angle in figure 9 indicate the presence of rather large losses in the vicinity of the rotor tip at the higher speeds, with no clearly defined minimum value of loss coefficient. At all the radial stations the low-loss region of operation occurred at higher incidence angles as the speed increased. In general, between the 50- and 83-percent stations, conventional loss-incidence curves with minimum-loss coefficients were obtained at all speeds. Although the losses for the blade elements near the tip are higher than design, the values shown for this region are comparable to those of other double-circular-arc-blade compressor rotors operating at the same level of inlet relative Mach number and diffusion factor

(refs. 8 and 9). In a subsequent section the loss data of this report are compared with loss correlations presented in reference 6 for a number of circular-arc-blade transonic rotors.

At the higher speeds and at low incidence-angle values, the axial velocity ratios increased rapidly with a small reduction in incidence angle. The axial velocity ratios at design-speed and peak-efficiency operation were approximately 8 to 12 percent higher than the design value over the entire blade span. The presence of the sharp increase in axial velocity ratios at the lower incidence angles for corrected rotor speeds of 1300, 1200, and 1100 feet per second indicates the presence of choking in the compressor blade row, with subsequent accelerations to very high velocities. As might be expected at a corrected tip speed of 975 feet per second, the axial velocity ratio over the entire range of incidence angles was higher than the design value because of the low pressure ratio.

The variation of peak blade-element efficiencies for the several corrected tip speeds was largest at the 11-percent station. For blade sections closer to the hub the variation in peak efficiencies was reduced principally because the efficiency at the higher tip speeds increased with decrease in radius. Peak over-all compressor efficiency at design speed was obtained at an incidence angle approximately 1° higher than design in the tip region and 2° to 3° higher than design at all other radii. For the blade elements at the 11-, 17.5-, and 33.5-percent stations, the peak efficiency obtained was approximately 15 percentage points below the respective design values, a reflection of the discrepancy between the experimental and design values of losses for these blade sections. Near the hub, blade-element efficiencies above 0.90 were obtained at all values of corrected tip speed.

The deviation-angle curves indicate that for blade sections near the tip there appeared to be a Mach number effect on deviation angle. Increasing the inlet relative Mach number above about 1.10 at a fixed incidence angle resulted in an increase in the deviation angle. In general, in the choked-flow region of incidence angle, an increase in deviation angle occurred as the back pressure was reduced.

At design speed and in the peak-efficiency range of incidence angles, the work coefficient in the tip region was higher than the design value. This was believed to be due to the higher than design camber angle in this region of the blade. The additional camber was apparently enough to overcome the higher than design axial velocities, which would ordinarily have resulted in a reduction in work input to the air. Although the design value of work input was obtained and even exceeded for some operating conditions at design speed, the large losses accompanying performance at these points caused relatively low efficiencies particularly in the tip region of the blade. The variation of work coefficient

with speed in the unchoked incidence-angle range was largest in the tip portion of the blade, while near the hub the work coefficient was about constant for all values of corrected tip speed.

The largest values of diffusion factor occurred in the tip region of the blades over the range of corrected tip speeds investigated. The diffusion factors at a corrected tip speed of 1200 feet per second were generally higher than at any of the other speeds tested for incidence angles corresponding to unchoked compressor operation. A comparison of the curves of relative total-pressure-loss coefficient for corrected tip speeds of 1300 and 1200 feet per second and for blade elements operating at supersonic relative inlet Mach numbers showed that the level of relative total-pressure-loss coefficient was generally higher at the higher speed. It seems evident that this increase in losses at design speed is a Mach number effect, because, in general, the axial velocity ratio was higher and the diffusion factor lower at design speed than at a corrected tip speed of 1200 feet per second. In the vicinity of the compressor over-all peak-efficiency point at design speed (point B, fig. 5) the design values of diffusion factor were approximated over about the outer half of the blade span. Near the hub the design values of diffusion factor were not obtained. At the 67-percent station, for example, the diffusion factors obtained near the over-all peak-efficiency point were about half the design value.

The recovery ratio, or reaction as it is sometimes called, is included on the blade-element plots because it is felt that, for high Mach number blade elements, with attendant shock waves on the suction surface of the blade, the assumptions surrounding the development of the diffusion factor may in some cases be violated. In such instances the static-pressure increase may serve as a useful loading criterion if some means is found for estimating the local shock strength. The curves (fig. 9) show that the variation of the recovery ratio with incidence angle was quite similar at corrected tip speeds of 1300, 1200, and 1100 feet per second for all radial stations. A slight difference in the variation can be seen at a tip speed of 975 feet per second, where the increase in recovery ratio with incidence angle is not so steep. For the three higher speeds the curves at each radial station reached a maximum and then decreased slightly as the incidence angle increased. At the lowest speed no decrease was observed with increasing incidence angle. The maximum value of recovery ratio obtained at each speed increased with a reduction in the streamline radius. The curves also show that for all radial stations the highest maximum value of the recovery ratio was obtained at a corrected tip speed of 1100 feet per second.

DISCUSSION OF RESULTS

The more important of the performance characteristics of this compressor at design speed may be stated as follows:

(1) The experimental blade-element relative total-pressure-loss coefficients in the vicinity of design incidence were considerably greater than the design values except for the blade section closest to the hub.

(2) The compressor choked at incidence angles approximately equal to the design values over the entire blade height except near the hub. At the hub the choked-flow incidence angle was about 1.5° greater than the design value.

In the following sections of this report these conditions are examined and an analysis of their effects on compressor performance is presented together with some considerations of the applicability of the radial-equilibrium concept to compressors of the type reported herein. In addition, the data of this investigation are applied to the correlation plots of incidence angle, deviation angle, and relative total-pressure-loss parameter of reference 6 to aid in the future extension of the empirical design rules and correction factors for double-circular-arc blades to higher Mach number levels.

Comparison with Design

An attempt was made to evaluate the effect of an increase in loss-coefficient level on the axial velocity ratio across a rotor blade row. The one-dimensional continuity equation was applied to the design inlet data at the mean radius, and calculations were carried out over a range of loss-coefficient values to determine the corresponding outlet axial velocities. It was assumed in the calculations that the outlet relative flow angle remained constant at the design value for the entire range of loss coefficients assumed. The selection of this particular value of outlet relative flow angle is somewhat arbitrary and serves only to illustrate the changes in design performance to be expected from a change in the loss-coefficient level. It must be emphasized that this method of approach does not consider any effects of radial variations of any flow parameters and is intended to show only the influence of the average level of total-pressure-loss coefficient on the average level of axial velocity ratio.

The derivation of the equation used in these calculations is presented in appendix B, and the results of the calculations are shown in figure 10 as the variation of axial velocity ratio and relative outlet Mach number with total-pressure-loss coefficient. Also shown in figure 10 are the design mass-averaged values of axial velocity ratio and relative outlet Mach number plotted at the design mass-averaged value of loss coefficient. In addition, the corresponding mass-averaged parameters for the experimental data of point A at design speed (fig. 5) are also included in the figure. In general, for this particular data point, the compressor was operating nearest to design inlet conditions, and the

radial variation of the outlet relative flow angle was approximately the same as specified in the design, especially in the mean and tip regions of the blade.

The two points plotted on the curve of axial velocity ratio in figure 10 are reasonably in accord with those computed from the one-dimensional approach; but, more important, the computed increase in axial velocity ratio predicted for an increase in loss coefficient conforms quite accurately with the experimental increase. Somewhat better agreement among the computed, design, and experimental values was obtained on the basis of the relative outlet Mach number.

The computed curves illustrate the penalty to be paid in increased axial velocity ratio, and therefore decreased work input, when the loss coefficients are greater than anticipated. The combination of reduced work input and higher losses results in a considerable reduction in efficiency. Calculations based on the one-dimensional Euler equation showed that, for the increase in axial velocity ratio and loss coefficient indicated by the data points of figure 10, the work coefficient was reduced by approximately 17 percent, the total-pressure ratio was reduced by about 11 percent, and the adiabatic efficiency was lowered by 13 percentage points. It is evident, therefore, that, to obtain design energy input at design turning angle in compressors operating at high speeds and high relative inlet Mach numbers, the values of loss coefficient must be known considerably more accurately than they were in the design of the present compressor. Conversely, the sensitivity of compressors of this type to errors in design assumptions of losses is much greater than that of machines with lower inlet relative Mach numbers.

Choking Analysis

It has been shown previously that the compressor choked prematurely and prevented the attainment of a total-pressure ratio at or near the design value at design weight flow. The blade-element performance curves show that a rise in relative total-pressure-loss coefficient occurred in the vicinity of the hub as the incidence angle was decreased from the value corresponding to minimum loss. This is regarded as evidence of flow choking.

In the design of this compressor, the possibility of flow choking in the hub region was investigated by determining, from a layout of the blade, the variation of blade passage width with blade chord. In an attempt to account for the three-dimensional nature of the flow, these passage widths were corrected by the amount of annulus contraction at each station along the blade chord. Flow choking was assumed to be imminent if at any point inside the blade passage the geometric area

was equal to the isentropic critical area of the flow far upstream of the compressor blade element. Based on this concept, flow choking should not have occurred at the hub section of this compressor at incidence angles equal to or higher than the design value.

This phase of the design technique, however, did not, for example, take into consideration any buildup of boundary layer along the blade surface and the annulus walls. In addition, no account was taken of the loss in total pressure that must occur as the flow is turned through the incidence angle and assumes a direction more or less guided by the inlet portion of the blades (refs. 17 and 18). Further, the flow between blades was assumed to be at a uniform velocity, which is certainly not true for the curving blade passages, especially near the hub where the camber is relatively large. These factors would all tend to increase the choking incidence angle, since they have the effect on the flow in the blade passage of respectively decreasing the geometric throat area, increasing the entropy, and decreasing the average mass flow. Still another factor, radial shift of mass flow inside the blade passage, would tend to increase the choking incidence angle at the hub if the shift were toward the inner wall of the annulus.

On the other hand, two effects would act to decrease the incidence angle and increase the value of maximum weight flow. First, the energy addition to the air in the rotating passage due to the radius change between the blade inlet and the geometric minimum section might result in an increase in air density at the minimum area and therefore an increase in the mass flow. Secondly, the hub curvature near the blade-inlet region was such (concave-looking from the casing) as to cause some reduction in velocity along streamlines near the hub and might therefore tend to reduce local velocity peaks ahead of the minimum area (e.g., acceleration around the leading edge of the blades on the suction surface, a contributing factor to increasing nonuniformity of flow at the choke point). The net result of the effects of all these conditions could not be evaluated except by the obvious method of examining the experimental data, where it seems clear that the preponderant influences must have been those which tended to produce choking at an incidence angle greater than the design value and therefore decrease the maximum weight flow to a value less than prescribed in the design.

A calculation was made in an attempt to evaluate one of the neglected factors described previously. It was assumed that the losses encountered by the air in turning through the incidence angle of 9° (experimental incipient-choke incidence angle for the blade section at $r_3 = 4.50$ in.) could be obtained from the equations developed in reference 18. As shown in reference 18 the resultant computed loss is the maximum loss to be expected for uniform flow inside the blade passage

at the leading edge and therefore may be pessimistic as far as applicability to the flow in this compressor is concerned. It may, however, serve as a useful criterion and was therefore used herein. The blade section $r_3 = 4.50$ inches was selected because it represented the section closest to the hub that could be traced mechanically to a large scale. From this blade trace the minimum geometric area (geometric throat) corrected for annulus contraction was found to occur inside the blade passage about 0.50 inch downstream of the rotor blade leading edge. The loss in relative total pressure due to the induction process into the blade passage (ref. 18), which was expressed as a fraction of the difference between the experimental inlet relative total and static pressures, was found to be approximately 0.086. This loss in total pressure resulted in a value of isentropic critical area about 0.95 of the geometric area. The calculation was repeated for the design inlet Mach number and incidence angle, and the ratio of isentropic critical area to the geometric area was about 0.99.

From these calculations it might be suspected that in the design case the allowance for such things as boundary-layer thickness and non-uniform flow of approximately 1 percent of the geometric throat area was insufficient. No recommended value of the ratio of isentropic critical area ahead of the minimum geometric area to the actual geometric minimum area can be stated at the present time, but it is possible that further analysis of other compressor rotors may yield useful information on the proper incidence angles to be used in the vicinity of the hub to avoid premature choking.

Radial Equilibrium

Reference 19 shows that for inviscid, axisymmetric, steady flow the radial component of the equation of motion for the flow at a station behind the rotor of this compressor may be written in two forms:

$$Jgc_p \frac{\partial T}{\partial r} = gt \frac{\partial S}{\partial r} + v_\theta \frac{\partial v_\theta}{\partial r} + \frac{v_\theta^2}{r} + v_z \frac{\partial v_z}{\partial r} - v_z \frac{\partial v_r}{\partial z} \quad (8)$$

$$v_r \frac{\partial v_r}{\partial r} + v_z \frac{\partial v_r}{\partial z} - \frac{v_\theta^2}{r} = - \frac{g}{\rho} \frac{\partial p}{\partial r} \quad (9)$$

In general, the radial velocity component v_r is not measured by conventional axial-flow-compressor instrumentation, since it is considered to be small. If it can be further assumed that the radial and axial

gradients of radial velocity are similarly negligible, then equations (8) and (9) may be written, respectively, as

$$Jg c_p \frac{\partial T}{\partial r} = g t \frac{\partial S}{\partial r} + V_\theta \frac{\partial V_\theta}{\partial r} + \frac{V_\theta^2}{r} + V_z \frac{\partial V_z}{\partial r} \quad (10)$$

$$\frac{g}{\rho} \frac{\partial p}{\partial r} = \frac{V_\theta^2}{r} \quad (11)$$

Equation (10) was developed in reference 19 into a form that facilitated computation of the radial variation of axial velocity. Equation (11) is the same form of the equation of motion as was used in the design of the compressor of this report. Within the restrictions of the assumptions made, both equations (10) and (11) were found to yield the same results for the radial variation of axial velocity when experimental values of total temperature, total pressure, and absolute flow angle at each of the several radial survey stations were substituted into them. The procedure used in carrying out the calculations when using equation (10) is given in reference 19; for equation (11), a slight modification to the method described in the design section of this report was used.

The calculated variation of axial velocity for three values of corrected weight flow at design speed is shown in figure 11, and the corresponding experimental values are included in the figure. The ordinate is made dimensionless by dividing it by the rotor tip speed at the inlet. Good agreement with the data was obtained at the lowest weight flow at all radii, and as the flow increased the agreement was still quite good except near the hub. In the vicinity of the hub, therefore, significant errors must have been introduced by one or more of the simplifying assumptions mentioned previously.

Two of the assumptions made in the development of the equation of motion as given in equation (10) were axial symmetry ($\partial/\partial\theta = 0$) and negligible radial-flow term ($V_z \frac{\partial V_r}{\partial z} = 0$). The assumption of axial symmetry is difficult to evaluate from stationary instrumentation such as used in this investigation, and recourse must be made to an intuitive approach. For example, references 2, 9, 20, and 21 found that the radial-equilibrium expressions in the form of either equation (10) or (11) of this report were adequate in describing the outlet axial velocity distributions of these transonic rotors. Since both of these equations assume axial symmetry, it might be postulated in the light of this evidence that the assumption is valid for a group of compressors of generally similar design and geometry operating under approximately the same conditions, including the rotor of the present investigation.

The compressor investigation of reference 8, however, showed that the radial-equilibrium expression of the form given by equation (10) did not fit the data in the vicinity of the hub. The reason advanced for the discrepancy was that the radial-flow term was not zero. Investigation of several transonic single-stage compressors reveals that the curvature of the hubs (roughly indicated by the slope of a line joining the hub radii at the inlet and outlet) of the rotors of references 2, 9, 20, and 21 was comparatively small, while the rotor hub curvature in reference 8 was considerably larger. The rotor hub curvature of the present investigation was about halfway between these two curvature regions and evidently was sufficiently great that the radial-flow term assumed importance. Consequently, it may be concluded that the principal source of disagreement between the calculated and experimental variations of axial velocity (fig. 11) can be ascribed to the assumption

that $V_z \frac{\partial v_r}{\partial z} = 0$. A method for evaluating this term accurately is necessary if agreement with experimental data is to be achieved for compressors with high pressure ratios, low hub-tip radius ratios, and short axial lengths. It may be noted that, in the case of a multistage compressor where it is customary for stages of this type to be used, the importance of the radial-flow term may not be so great, since the flow would not be returned to the axial direction in the short length characteristic of this single-stage test setup.

Extension of Double-Circular-Arc-Blade Data Correlation

As pointed out previously, the primary purpose of this investigation is to determine the performance of a double-circular-arc-blade rotor in a region of relative inlet Mach number for which little information is available. As a corollary to this purpose, it is of interest to apply the data obtained to the correlations presented in reference 6, where current information on a number of compressor rotors was assembled with the view of establishing suitable corrections to the two-dimensional-cascade rules developed in reference 22. The factors considered in reference 6 are incidence angle, deviation angle, and a relative total-pressure-loss parameter. The correlation plots for these quantities are presented for three blade elements of each of a number of compressors operating at or near their incidence angles for minimum relative total-pressure-loss coefficient.

The double-circular-arc-blade transonic rotor data of reference 6 for three blade elements denoted as tip, mean, and hub are reproduced in figures 12 to 15, and the data of the present report for the 11-, 50-, and 83-percent stations are added. This method of presenting the data was chosen because it was felt that, in view of the limited amount of additional data available, any attempt to revise the proposed

correction curves (figs. 21 to 23 of ref. 6) would be premature. It should be noted that, for the data of this report, in many cases no minimum value of blade-element relative total-pressure-loss coefficient was obtained (e.g., fig. 9(a) for corrected tip speeds of 1100, 1200, and 1300 ft/sec). In these instances, several points in the vicinity of the lowest value of loss coefficient were used on the correlation plots. Where a clearly defined value of minimum-loss coefficient was obtained, only one point appears on the plots for a particular radial position and corrected tip speed.

4001 The correlation plots of total-pressure-loss parameter against diffusion factor (fig. 12) indicate that in the tip and hub sections the data of this report are generally within the spread of data presented in reference 6. At the mean-radius section the points for corrected tip speeds lower than the design value also appear to correlate with the reference data, but at design speed the loss-parameter values are appreciably higher.

The spread of data for this compressor in the tip region seems to be a function of the corrected tip speed (inlet relative Mach number), since it can be observed that, in general, as the speed increased the value of loss parameter increased at a fixed value of diffusion factor. Evidently, the diffusion-factor concept is not sufficiently adequate to completely describe the blade-loading phenomenon in this instance. A more fundamental quantity affecting the losses in this case may be the blade suction-surface Mach number, which, based on a simplified analysis, is a function of relative inlet angle, solidity, and blade curvature (refs. 23 and 24). Computations carried out for the rotor of this report using the procedure given in reference 23 indicated that, for design-speed operation, tip-region blade surface Mach numbers of the order of 1.7 to 1.9 were obtained. Because of the increased incidence angle, higher values of blade surface Mach numbers were obtained at the peak-pressure-ratio operating condition. A blade surface Mach number effect may also be the cause of the increase in loss parameter obtained at the mean radius at design-speed operation mentioned previously. Reference to figure 9(d) shows that only at design speed were appreciably supersonic relative inlet Mach numbers obtained. Comparison with the low-loss high-speed mean-radius data of reference 9, which were at a slightly lower inlet relative Mach number, shows that the loss-parameter value of that rotor configuration was very close to the values shown for the rotor of this investigation. This admittedly small amount of evidence indicates that the presence of supersonic relative inlet Mach numbers at this radial position with attendant accelerations on the suction surface of the blade can result in significant increases in the local value of total-pressure-loss parameter.

In the incidence-angle correlation plots of figure 13 the ordinate expresses the difference between the experimental incidence angle at or near minimum loss and the calculated minimum-loss incidence angle for a

CONFIDENTIAL

two-dimensional cascade having the same blade shape, relative inlet angle, and solidity. It represents, then, a measure of the correction necessary before applying the design rules of reference 22 to a compressor design and is shown as a function of the relative inlet Mach number. Figure 13 indicates that no significant alteration to the general trend of the data from reference 6 is obtained by the addition of the data of this report. It appears that at the tip section the incidence-angle correction for relative inlet Mach numbers between 1.1 and 1.3 is about constant at 4° . More information is needed, however, before any definite recommendation can safely be made for this and the other blade elements.

The deviation-angle corrections to the two-dimensional design rules are plotted in figures 14 and 15 for two methods of computing the two-dimensional deviation angle. In figure 14 the two-dimensional deviation angle is computed by the method outlined in reference 22, and in figure 15 it is computed by Carter's rule (ref. 13). For the data of this report the use of Carter's rule resulted in three-dimensional deviation-angle corrections that were about 0.5° to 1.0° higher than those calculated from the cascade rule of reference 22 for the three radial positions shown. In general, the extensions to the correlation plots provided by the information gained from the present investigation showed no important changes at higher Mach numbers. There seems to be an indication at the highest Mach number tested that the two-dimensional and three-dimensional deviation angles at the mean-radius position are about the same. This is especially true of the correlation based on Carter's rule (fig. 15), not only at the mean radius but also for the blade element near the tip.

SUMMARY OF RESULTS

From the performance investigation of a double-circular-arc-blade transonic axial-flow-compressor rotor designed to operate at tip relative Mach numbers up to 1.37, the following results were obtained:

1. The lowest values of relative total-pressure-loss coefficient obtained at design speed were considerably greater than the design values over most of the blade span.
2. The outlet axial velocities at design speed were, on the average, appreciably higher than the design values over the entire range of compressor weight flow.
3. The compressor choked prematurely and prevented the attainment of design total-pressure ratio at or near the design weight flow.
4. Underestimation of the magnitude of the relative total-pressure-loss coefficients in the design of the compressor caused a significant increase in the outlet axial velocity. Because of the sensitivity of

compressors of this Mach number range to errors of this type, appreciable reductions in work input, total pressure, and adiabatic efficiency occurred when the compressor was operated near design incidence angle at design speed.

5. The isentropic one-dimensional-flow equation does not satisfactorily predict the choking incidence angle in the vicinity of the rotor hub. Consideration should be given to the induction loss encountered by the air in entering the blade row when specifying the design values of incidence angles near the hub.

6. The concept of simple radial equilibrium with entropy gradients was adequate except in the vicinity of the blade hub, where the curvature of the inner wall assumed importance. A method of evaluating the radial-flow term of the equilibrium equation is desirable for compressors with low hub-tip radius ratios, high pressure ratios, and short axial lengths.

7. The data of this report were applied to the correlation plots of corrections to the two-dimensional rule values of incidence and deviation angles and to the loss-parameter plots of a collection of double-circular-arc-blade transonic-compressor investigations. The data served to extend the plots to higher relative inlet Mach numbers but did not significantly change the correlations of incidence- and deviation-angle corrections. Evidence was believed present indicating an effect of blade suction-surface Mach number on total-pressure-loss parameter at constant diffusion factor at both the tip- and mean-radius blade elements.

Lewis Flight Propulsion Laboratory
National Advisory Committee for Aeronautics
Cleveland, Ohio, May 1, 1956

APPENDIX A

SYMBOLS

A	area, sq ft
a	speed of sound, ft/sec
c_p	specific heat at constant pressure, Btu/(lb)(°R)
D	diffusion factor
g	acceleration due to gravity, 32.17 ft/sec ²
H	total enthalpy
$\frac{\Delta H}{U_t^2}$	dimensionless work coefficient
i	incidence angle, angle between relative inlet-air direction and tangent to blade mean camber line at leading edge, deg
J	mechanical equivalent of heat, 778.2 ft-lb/Btu
K_{bk}	blockage factor
M	Mach number
P	total pressure, lb/sq ft
p	static pressure, lb/sq ft
R	gas constant, 53.35 ft-lb/(lb)(°R)
r	radius from center of rotation, in.
S	entropy, ft-lb/(lb)(°R)
T	total temperature, °R
t	static temperature, °R
U	rotor speed, ft/sec
V	fluid velocity, ft/sec
w	weight flow, lb/sec

x	percent of passage height
z	axial distance
β	air angle, angle between air velocity and axial direction, deg
$\Delta\beta$	air-turning angle, inlet-air angle minus outlet-air angle, deg
γ	ratio of specific heats
δ	ratio of inlet total pressure to NACA standard sea-level pressure of 2116 lb/sq ft
δ°	deviation angle, angle between relative outlet-air direction and tangent to blade mean camber line at trailing edge, deg
η_{ad}	adiabatic efficiency
Θ	angular coordinate
θ	ratio of total temperature to NACA standard sea-level temperature of 518.7° R
α	blade angle, angle between tangent to blade mean camber line at leading or trailing edge and axial direction, deg
ρ	static density, lb/cu ft
σ	solidity, ratio of chord to spacing
ϕ	blade camber angle, difference between blade angles at leading and trailing edges, deg
\bar{c}_w	total-pressure-loss coefficient

Subscripts:

a	stagnation value of a quantity
b	blade element
C	refers to compressor performance data
F	frontal
h	hub
id	ideal

m.a. mass-averaged value

r radial direction

t tip

z axial direction

θ tangential direction

1 inlet tank

2 upstream of rotor; location of static-pressure survey rake

2-D refers to values determined from the two-dimensional design rules
of ref. 22

3 rotor inlet

4 rotor outlet

Superscript:

' relative to rotor

APPENDIX B

EFFECT OF VARIATIONS IN RELATIVE TOTAL-PRESSURE-LOSS

COEFFICIENT ON OUTLET AXIAL VELOCITY

The performance data of this report show that the compressor could operate at about the design inlet condition. Also, for this point of operation the design value of relative turning angle at the mean outlet radius was approximately obtained. However, the experimental levels of relative total-pressure-loss coefficient and axial velocity ratio were higher than the design values at this operating point, and the compressor efficiency and work input were low. It was decided, therefore, to attempt to evaluate the effect on performance of varying the level of loss coefficient for fixed inlet conditions and relative turning angle.

The computations were carried out at the mean-radius station both because of the performance characteristics mentioned above and because this station could be considered as representing a kind of average condition at the rotor inlet and outlet. A more comprehensive investigation would have involved calculations at several radial stations; but, since only a qualitative answer was desired, the additional effort was felt to be unnecessary. This is essentially, then, a one-dimensional approach to the flow through the compressor and disregards variations in flow parameters set up by considerations of radial equilibrium.

From the continuity equation applied between stations 3 and 4, the following expression is obtained:

$$\frac{V_{z,4}}{V_{z,3}} = \frac{\rho_3}{\rho_4} \frac{A_3}{A_4} \frac{K_{bk,3}}{K_{bk,4}} = \frac{M_4' \cos \beta_4' a_4}{M_3' \cos \beta_3' a_3} \quad (B1)$$

which may be written as

$$K_{bk,3} \frac{\rho_3}{\rho_{a,3}} \rho_{a,3}' A_3 M_3' \frac{a_3}{a_{a,3}'} a_{a,3}' \cos \beta_3' = K_{bk,4} \frac{\rho_4}{\rho_{a,4}} \rho_{a,4}' A_4 M_4' \frac{a_4}{a_{a,4}'} a_{a,4}' \cos \beta_4' \quad (B2)$$

From isentropic relations, the perfect gas law, and the conventional equation for velocity of sound,

$$\frac{\rho_3}{\rho_{a,3}'} = \left[1 + \frac{\gamma - 1}{2} (M_3')^2 \right]^{-\frac{1}{\gamma - 1}} \quad (B3)$$

$$\frac{a_3}{a'_{a,3}} = \left[1 + \frac{\gamma - 1}{2} (M'_3)^2 \right]^{-\frac{1}{2}} \quad (B4)$$

$$\rho'_{a,3} = \frac{P'_3}{RT'_3} \quad (B5)$$

$$a'_{a,3} = \sqrt{\gamma g R T'_3} \quad (B6)$$

Substituting equations (B3) to (B6) into (B2) and reducing yield

$$\frac{M'_3}{\left[1 + \frac{\gamma - 1}{2} (M'_3)^2 \right]^3} \frac{A_3}{A_4} \frac{K_{bk,3}}{K_{bk,4}} \frac{\cos \beta'_3}{\cos \beta'_4} \left(\frac{T'_4}{T'_3} \right)^{1/2} \frac{P'_3}{P'_4} = \frac{M'_4}{\left[1 + \frac{\gamma - 1}{2} (M'_4)^2 \right]^3} \quad (B7)$$

From the definition of relative total-pressure-loss coefficient as given in reference 12,

$$\bar{\omega}' = \frac{\left(\frac{P'_4}{P'_3} \right)_{id} - \frac{P'_4}{P'_3}}{1 - \frac{P'_3}{P'_3}}$$

or

$$\frac{P'_4}{P'_3} = \left(\frac{P'_4}{P'_3} \right)_{id} - \bar{\omega}' \left\{ 1 - \left[1 + \frac{\gamma - 1}{2} (M'_3)^2 \right]^{-\frac{\gamma}{\gamma - 1}} \right\} \quad (B8)$$

The substitution of equation (B8) into (B7) with the assumption that

$$\frac{T'_4}{T'_3} = \left(\frac{P'_4}{P'_3} \right)_{id}^{\frac{\gamma}{\gamma - 1}} = 1.0 \text{ (negligible radius change along the mean streamline through the rotor) gives}$$

$$\frac{\frac{M_3'}{1 + \frac{\gamma - 1}{2} (M_3')^2} \frac{A_3 K_{bk,3} \cos \beta_3'}{A_4 K_{bk,4} \cos(\beta_3' - \Delta\beta')}}{1 - \bar{\omega}' \left\{ 1 - \left[1 + \frac{\gamma - 1}{2} (M_3')^2 \right]^{-\frac{\gamma}{\gamma - 1}} \right\}} = \frac{M_4'}{\left[1 + \frac{\gamma - 1}{2} (M_4')^2 \right]^3} \quad (B9)$$

where

$$\Delta\beta' = \beta_3' - \beta_4'$$

Further, since

$$V_{z,3} = M_3' a_3 \cos \beta_3'$$

and

$$V_{z,4} = M_4' a_4 \cos \beta_4'$$

then,

$$\frac{V_{z,4}}{V_{z,3}} = \frac{M_4'}{M_3'} \frac{\cos(\beta_3' - \Delta\beta')}{\cos \beta_3'} \frac{\frac{a_4}{a_4'} \frac{a_{a,4}'}{a_{a,3}'}}{\frac{a_3}{a_3'} \frac{a_{a,3}'}} = \frac{M_4'}{M_3'} \frac{\cos(\beta_3' - \Delta\beta')}{\cos \beta_3'} \left[\frac{1 + \frac{\gamma - 1}{2} (M_3')^2}{1 + \frac{\gamma - 1}{2} (M_4')^2} \right]^{1/2} \quad (B10)$$

The solution to equation (B9) was obtained by a trial-and-error process where all conditions at the mean-radius inlet station were assumed known and equal to the design values. The relative turning angle $\Delta\beta'$ was assumed to be the design value at the mean radius. The design values of inlet and outlet blockage factors were used, since the experimental values compared quite closely. Values of M_4' obtained from the solution of equation (B9) were substituted into equation (B10) to obtain the corresponding values of axial velocity ratio. In solving equation (B9) for relative outlet Mach number, only the subsonic values were considered to be of interest, since the compressor was designed for this mode of operation. Because the approach advanced in the development of these equations is one-dimensional, the values of $\bar{\omega}'$ should be considered in this case as average values and not confined to the mean-radius station alone.

REFERENCES

1. Lieblein, Seymour, Lewis, George W., Jr., and Sandercock, Donald M.: Experimental Investigation of an Axial-Flow Compressor Inlet Stage Operating at Transonic Relative Inlet Mach Numbers. I - Over-All Performance of Stage with Transonic Rotor and Subsonic Stators Up to Rotor Relative Inlet Mach Number of 1.1. NACA RM E52A24, 1952.
2. Schwenk, Francis C., Lieblein, Seymour, and Lewis, George W., Jr.: Experimental Investigation of an Axial-Flow Compressor Inlet Stage Operating at Transonic Relative Inlet Mach Numbers. III - Blade-Row Performance of Stage with Transonic Rotor and Subsonic Stator at Corrected Tip Speeds of 800 and 1000 Feet Per Second. NACA RM E53G17, 1953.
3. Klapproth, John F.: General Considerations of Mach Number Effects on Compressor-Blade Design. NACA RM E53L23a, 1954.
4. Andrews, S. J.: Tests Related to the Effect of Profile Shape and Camber Line on Compressor Cascade Performance. Rep. No. R.60, British N.G.T.E., Oct. 1949.
5. Howell, A. R.: A Note on Compressor Base Aerofoils C.1, C.2, C.3, C.4, C.5, and Aerofoils Made Up of Circular Arcs. Memo. No. M.1011, Power Jets (Res. and Dev.), Ltd., Sept. 1944.
6. Robbins, William H., Jackson, Robert J., and Lieblein, Seymour: Blade-Element Flow in Annular Cascades. Ch. VII of Aerodynamic Design of Axial-Flow Compressors, Vol. II. NACA RM E56B03a, 1956.
7. Tysl, Edward R., Schwenk, Francis C., and Watkins, Thomas B.: Experimental Investigation of a Transonic Compressor Rotor with a 1.5-Inch Chord Length and an Aspect Ratio of 3.0. I - Design, Over-All Performance, and Rotating-Stall Characteristics. NACA RM E54L31, 1955.
8. Montgomery, John C., and Glaser, Frederick W.: Experimental Investigation of a 0.4 Hub-Tip Diameter Ratio Axial-Flow Compressor Inlet Stage at Transonic Inlet Relative Mach Numbers. II - Stage and Blade-Element Performance. NACA RM E54I29, 1955.
9. Robbins, William H., and Glaser, Frederick, W.: Investigation of an Axial-Flow-Compressor Rotor with Circular-Arc Blades Operating Up to a Rotor-Inlet Relative Mach Number of 1.22. NACA RM E53D24, 1953.

10. Klapproth, John F., Jacklitch, John J., Jr., and Tysl, Edward R.: Design and Performance of a 1400-Foot-Per-Second-Tip-Speed Supersonic Compressor Rotor. NACA RM E55A27, 1955.
11. Stanitz, John D.: Approximate Design Methods for High-Solidity Blade Elements in Compressors and Turbines. NACA TN 2408, 1951.
12. Lieblein, Seymour, Schwenk, Francis C., and Broderick, Robert L.: Diffusion Factor for Estimating Losses and Limiting Blade Loadings in Axial-Flow-Compressor Blade Elements. NACA RM E53D01, 1953.
13. Carter, A. D. S., and Hughes, Hazel P.: A Theoretical Investigation into the Effect of Profile Shape on the Performance of Airfoils in Cascade. R. & M. No. 2384, British A.R.C., Mar. 1946.
14. Anon.: Power Test Codes A.S.M.E. 1940. Information on Instruments and Apparatus. Pt. 5, Ch. 4, pub. by A.S.M.E., 1940.
15. NACA Subcommittee on Compressors: Standard Procedures for Rating and Testing Multistage Axial-Flow Compressors. NACA TN 1138, 1946.
16. Lewis, George W., Jr., Schwenk, Francis C., and Serovy, George K.: Experimental Investigation of a Transonic Axial-Flow-Compressor Rotor with Double-Circular-Arc Airfoil Blade Sections. I - Design, Over-All Performance, and Stall Characteristics. NACA RM E53L21a, 1954.
17. Wright, Linwood C.: Approximate Effect of Leading-Edge Thickness, Incidence Angle, and Inlet Mach Number on Inlet Losses for High-Solidity Cascades of Low Cambered Blades. NACA TN 3327, 1954.
18. Kramer, James C., and Stanitz, John D.: Prediction of Losses Induced by Angle of Attack in Cascades of Sharp-Nosed Blades for Incompressible and Subsonic Compressible Flow. NACA TN 3149, 1955.
19. Hatch, James E., Giamati, Charles C., and Jackson, Robert J.: Application of Radial-Equilibrium Condition to Axial-Flow Turbomachine Design Including Consideration of Change of Entropy with Radius Downstream of Blade Row. NACA RM E54A20, 1954.
20. Lewis, George W., Jr., and Schwenk, Francis C.: Experimental Investigation of a Transonic Axial-Flow-Compressor Rotor with Double-Circular-Arc Airfoil Blade Sections. II - Blade-Element Performance. NACA RM E54J08, 1955.

21. Schwenk, Francis C., and Tysl, Edward R.: Experimental Investigation of a Transonic Compressor Rotor with a 1.5-Inch Chord Length and an Aspect Ratio of 3.0. II - Blade-Element Performance. NACA RM E55F10, 1955.
22. Lieblein, Seymour: Experimental Flow in Two-Dimensional Cascades. Ch. VI of Aerodynamic Design of Axial-Flow Compressors, Vol. II. NACA RM E56B03a, 1956.
23. Schwenk, Francis C., and Lewis, George W., Jr.: Experimental Investigation of a Transonic Axial-Flow-Compressor Rotor with Double-Circular-Arc Blade Sections. III - Comparison of Blade-Element Performance with Three Levels of Solidity. NACA RM E55F01, 1955.
24. Tysl, Edward R., and Schwenk, Francis C.: Experimental Investigation of a Transonic Compressor Rotor with a 1.5-Inch Chord Length and an Aspect Ratio of 3.0. III - Blade-Element and Over-All Performance at Three Solidity Levels. NACA RM E56D06, 1956.

TABLE I. - ROTOR BLADE DESIGN VALUES AND GEOMETRY

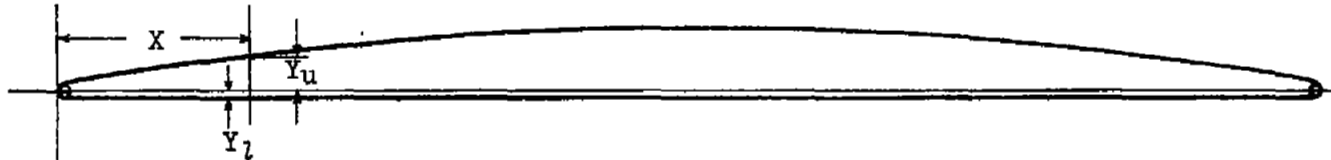
Passage height, percent	Streamline radius, in.		Inlet absolute Mach number, M_3	Inlet relative Mach number, M_3'	Inlet relative air angle, β_3' , deg	Incidence angle, i , deg
	Inlet, r_3	Outlet, r_4				
0 (tip)	8.000	7.750	0.634	1.366	62.36	3.00
20	7.200	7.119	.636	1.262	59.78	4.88
40	6.400	6.488	.630	1.156	56.89	5.94
60	5.600	5.856	.619	1.048	53.75	6.76
80	4.800	5.225	.606	.944	50.00	7.42
100 (hub)	4.000	4.594	.582	.837	46.00	8.00

Passage height, percent	Outlet absolute Mach number, M_4	Outlet relative Mach number, M_4'	Outlet relative air angle, β_4' , deg	Outlet absolute air angle, β_4 , deg	Work coefficient, $\frac{\Delta H}{U_{t,3}^2}$	Deviation angle, δ° , deg	Blade-element efficiency, $\eta_{ad,b}$	Diffusion factor, D
0 (tip)	0.648	0.901	53.24	33.60	0.310	3.32	0.855	0.445
20	.662	.850	49.24	33.10	.285	2.68	.908	.431
40	.670	.784	44.30	33.30	.264	2.71	.959	.414
60	.682	.710	37.90	35.10	.254	3.16	.970	.418
80	.700	.627	29.00	38.60	.251	3.93	.960	.436
100 (hub)	.740	.556	16.80	44.05	.257	5.01	.914	.526

CU-5 back

TABLE II. - COORDINATES OF TIP SECTION OF A ROTOR BLADE MEASURED
ON DESIGN STREAM SURFACE

[r_3 , 8.000 in.; r_4 , 7.750 in.; leading- and trailing-edge radii, 0.010 in.]



X	Y_u	Y_l	X	Y_u	Y_l
0	0	0	1.000	0.082	0.006
.100	.028	.014	1.100	.078	.006
.200	.041	.012	1.200	.076	.006
.300	.053	.010	1.300	.071	.006
.400	.063	.009	1.400	.065	.007
.500	.071	.009	1.500	.057	.010
.600	.077	.009	1.600	.046	.011
.700	.082	.009	1.700	.027	.012
.800	.084	.008	1.750	.009	.010
.900	.084	.007	1.762	0	0

4001 .

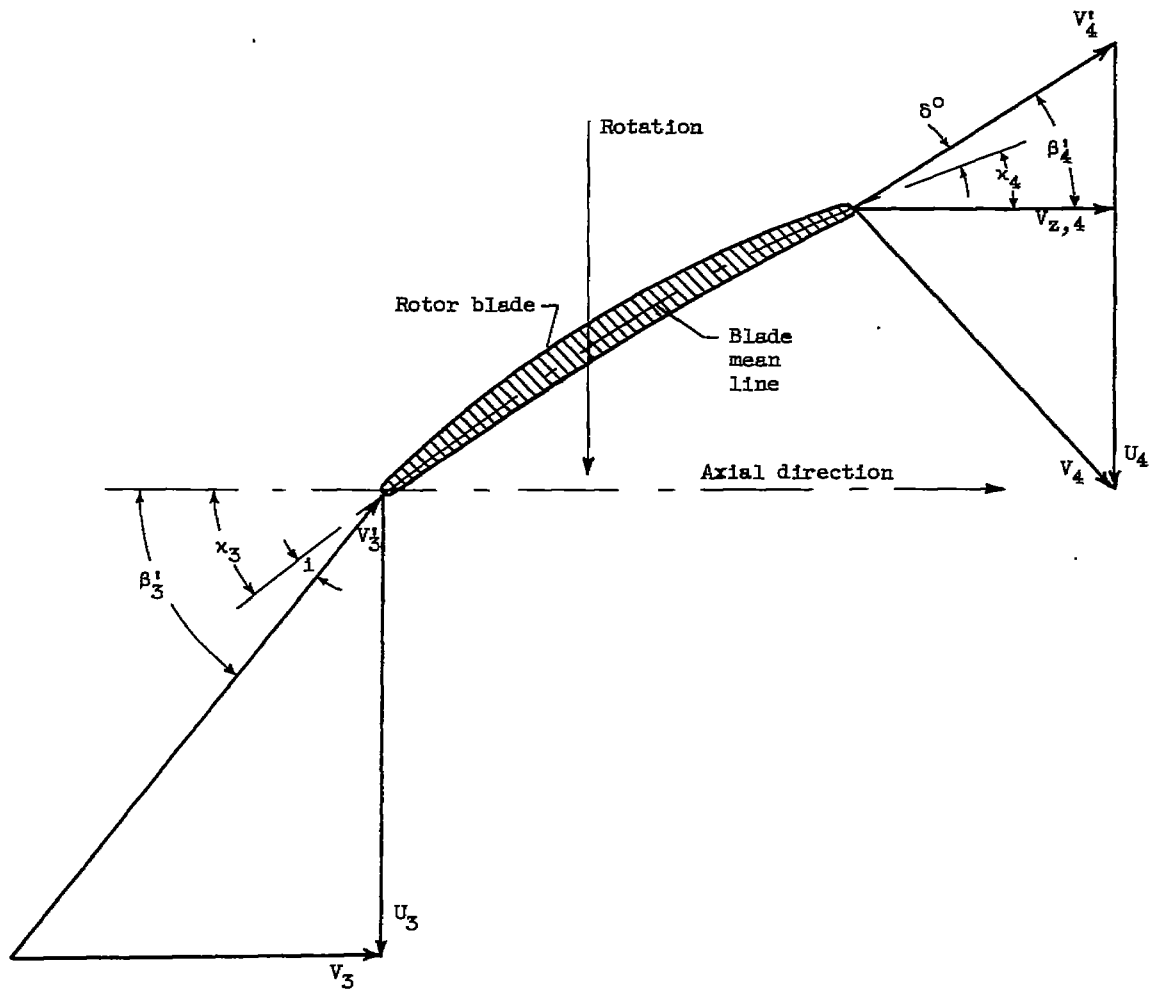


Figure 1. - Blade-element notation for typical blade section.

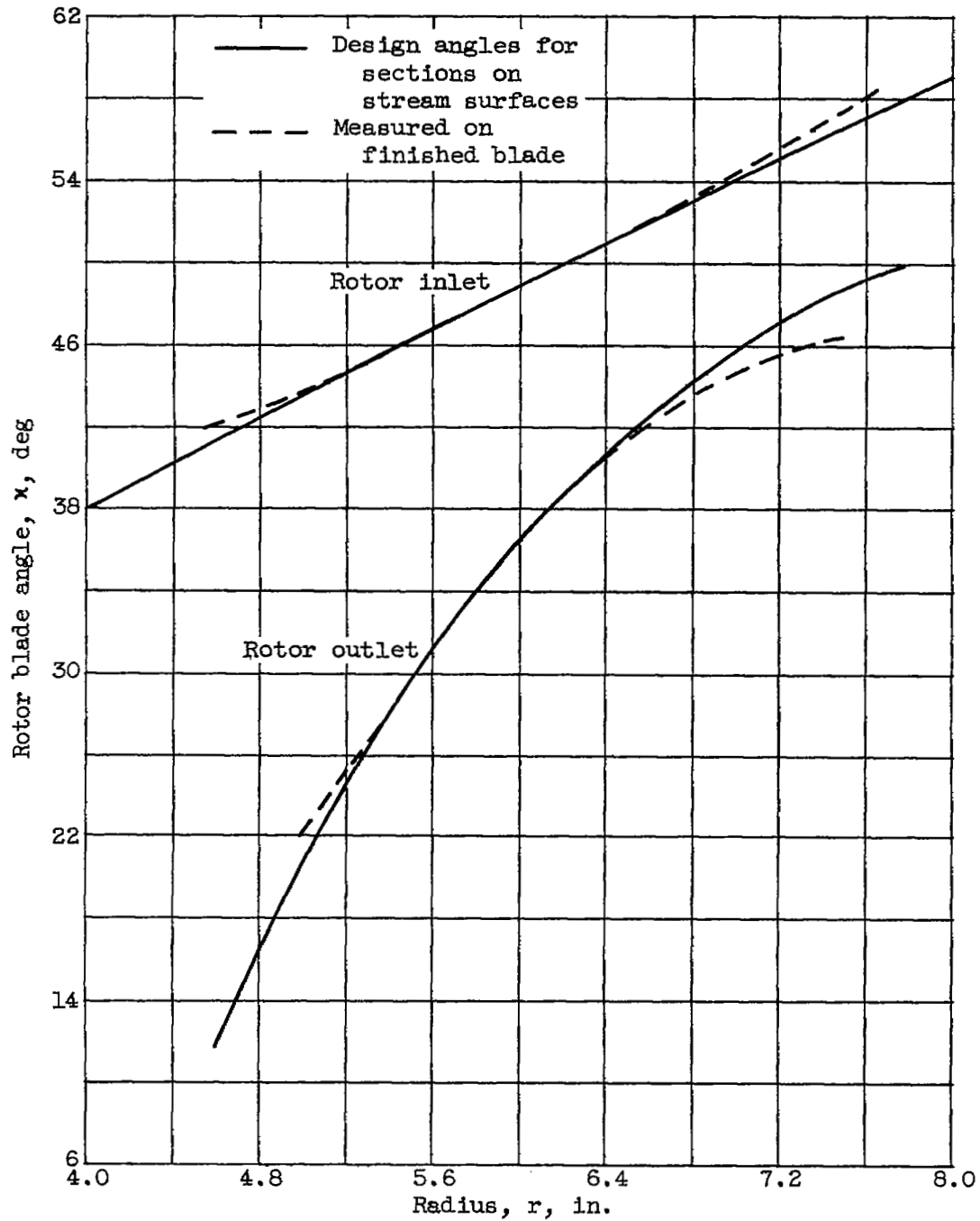
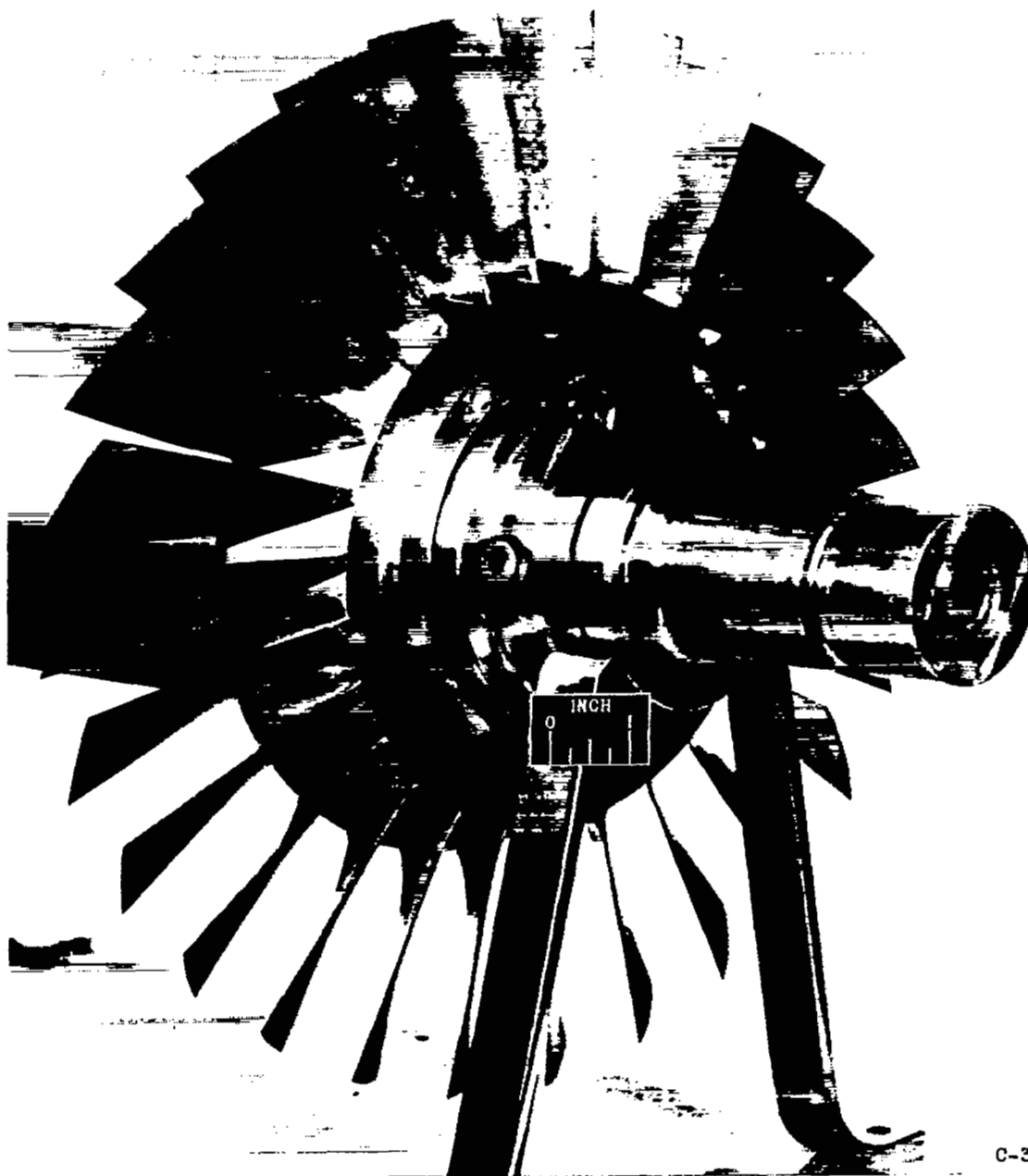


Figure 2. - Comparison of design and measured values of blade angles at rotor inlet and outlet.



C-39136

Figure 3. - Transonic-compressor rotor designed for tip speed of 1300 feet per second.

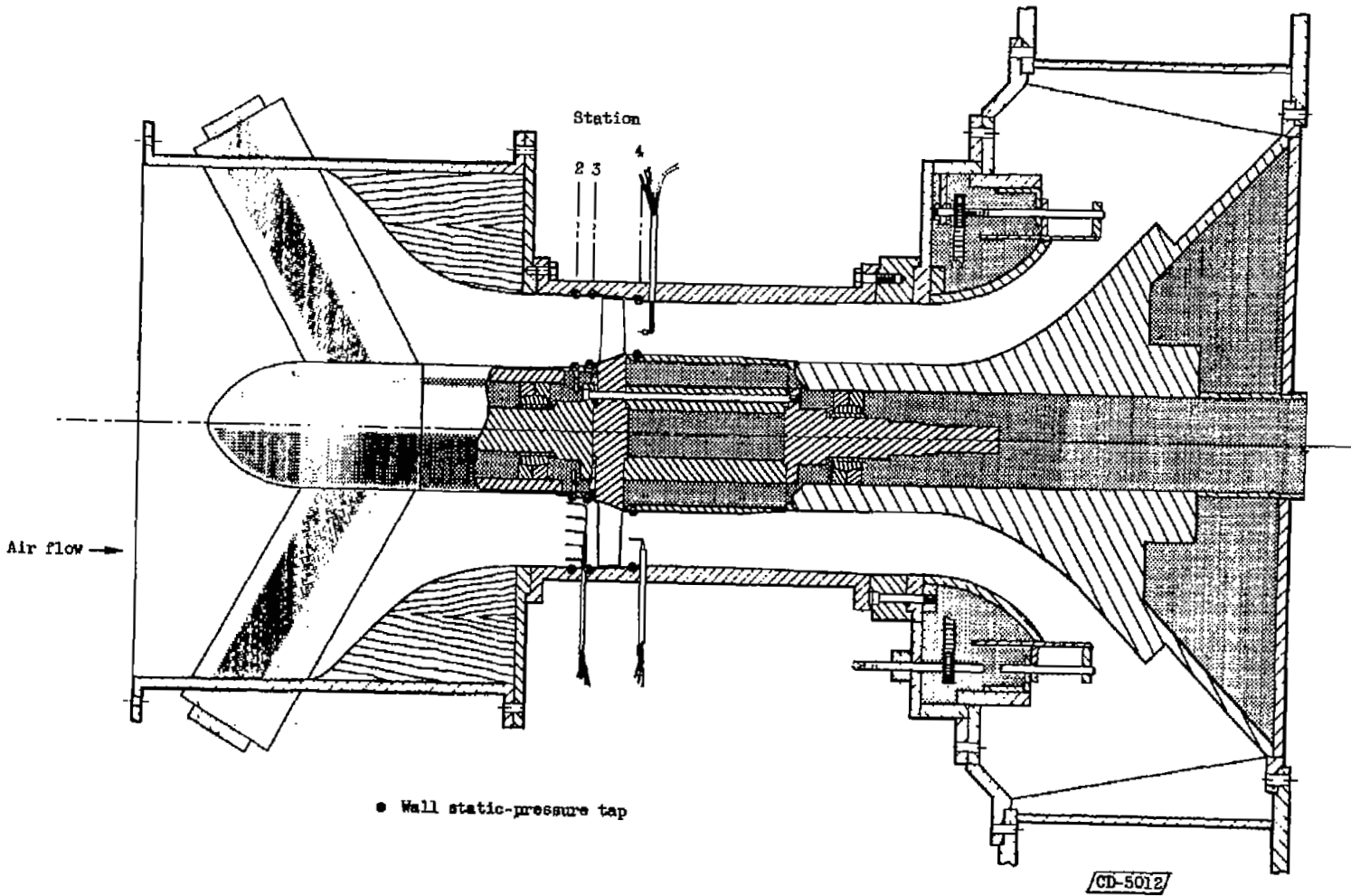


Figure 4. - Schematic diagram of test section of compressor installation.

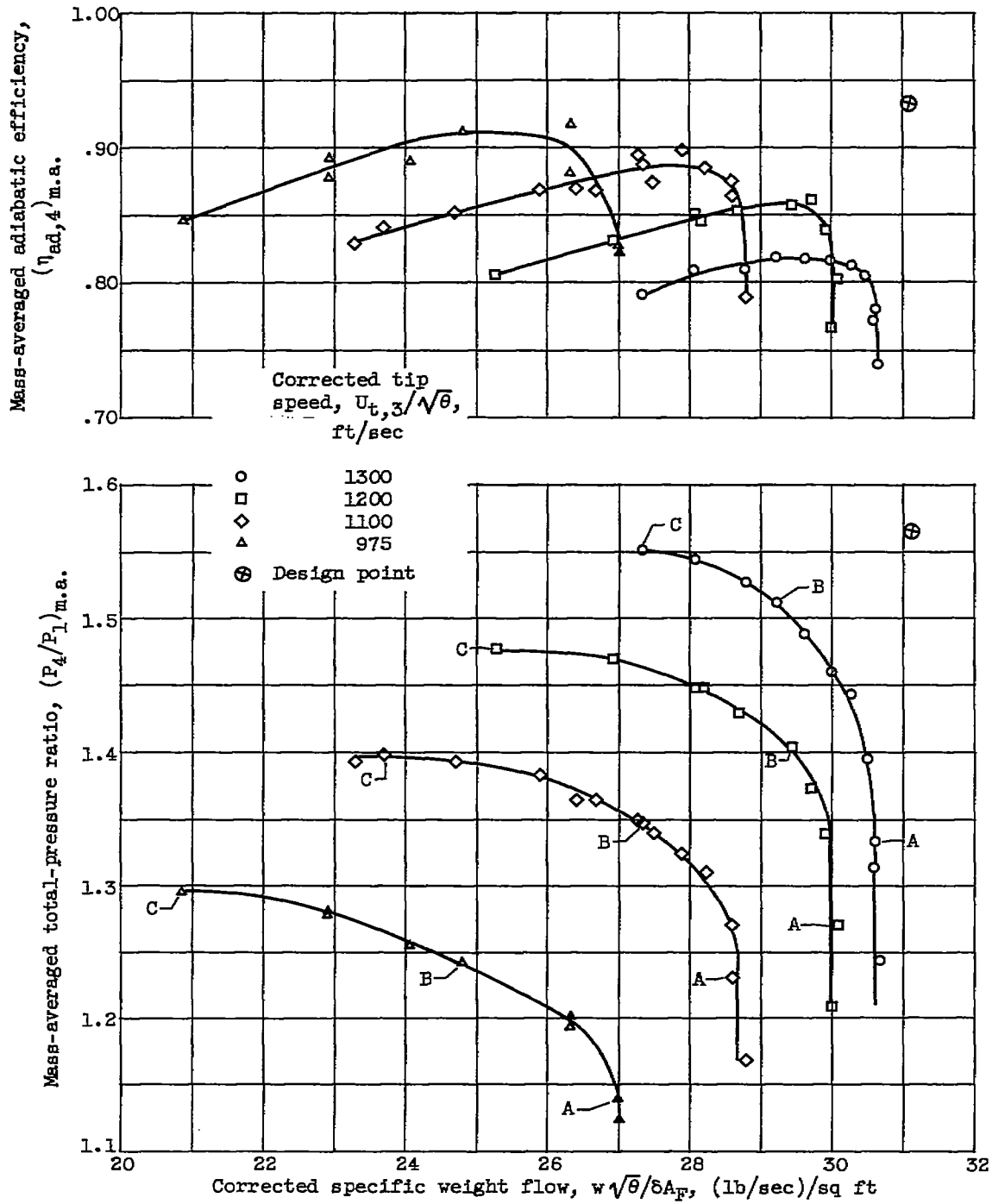
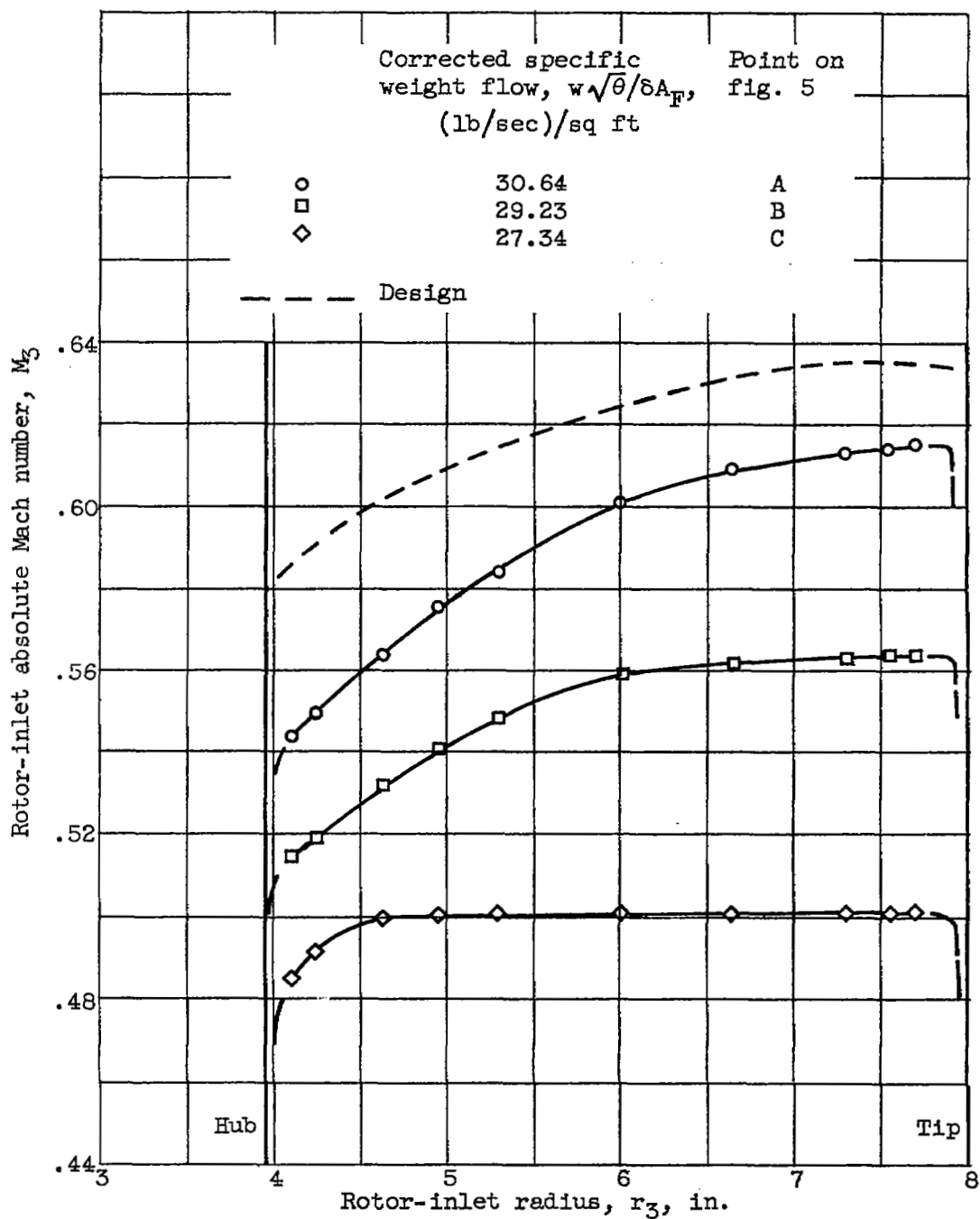
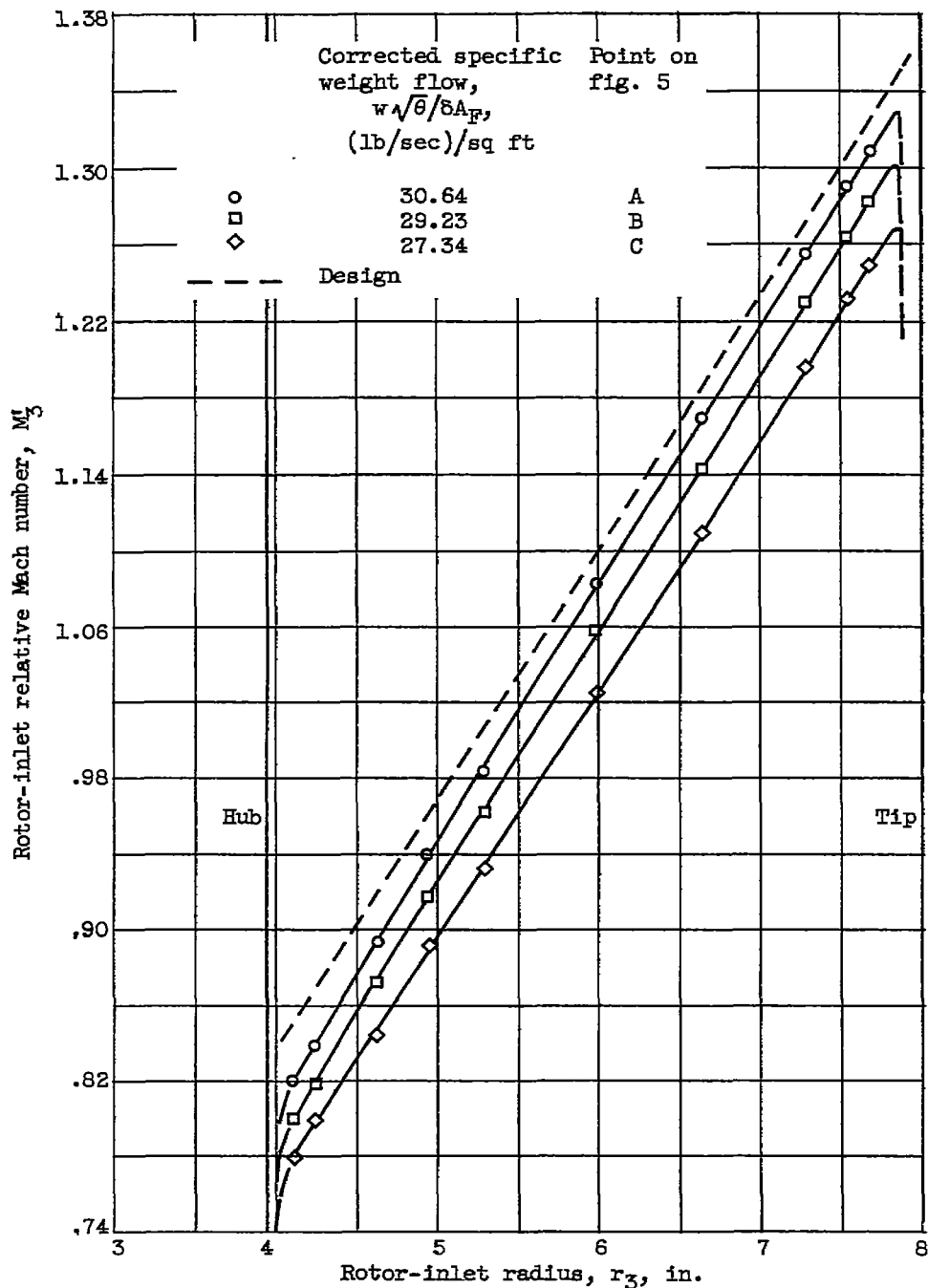


Figure 5. - Compressor over-all performance based on mass-averaged pressures and temperatures at station 4.



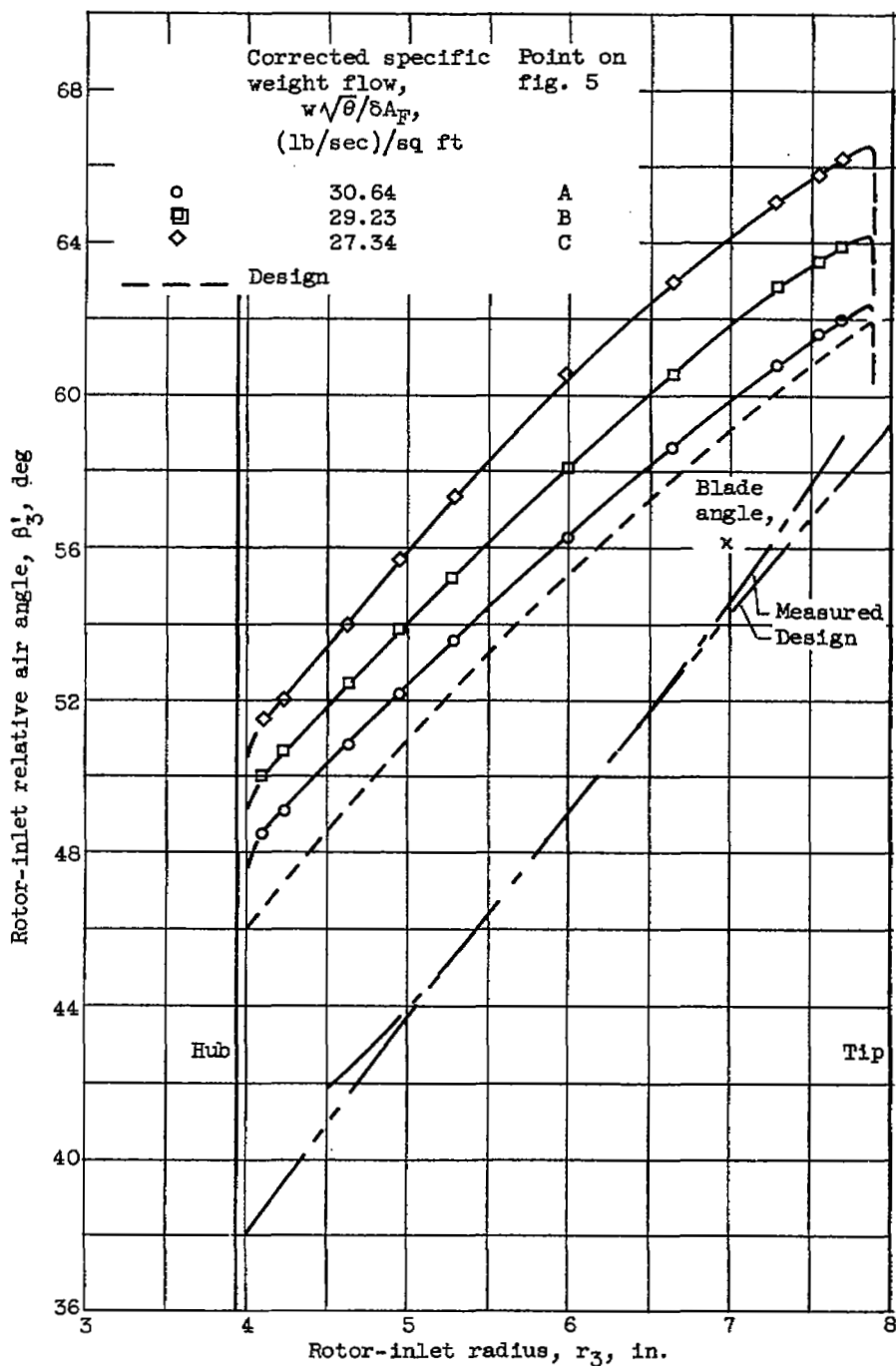
(a) Absolute inlet Mach number.

Figure 6. - Radial variation of rotor-inlet parameters at design speed for three values of corrected specific weight flow.



(b) Relative inlet Mach number.

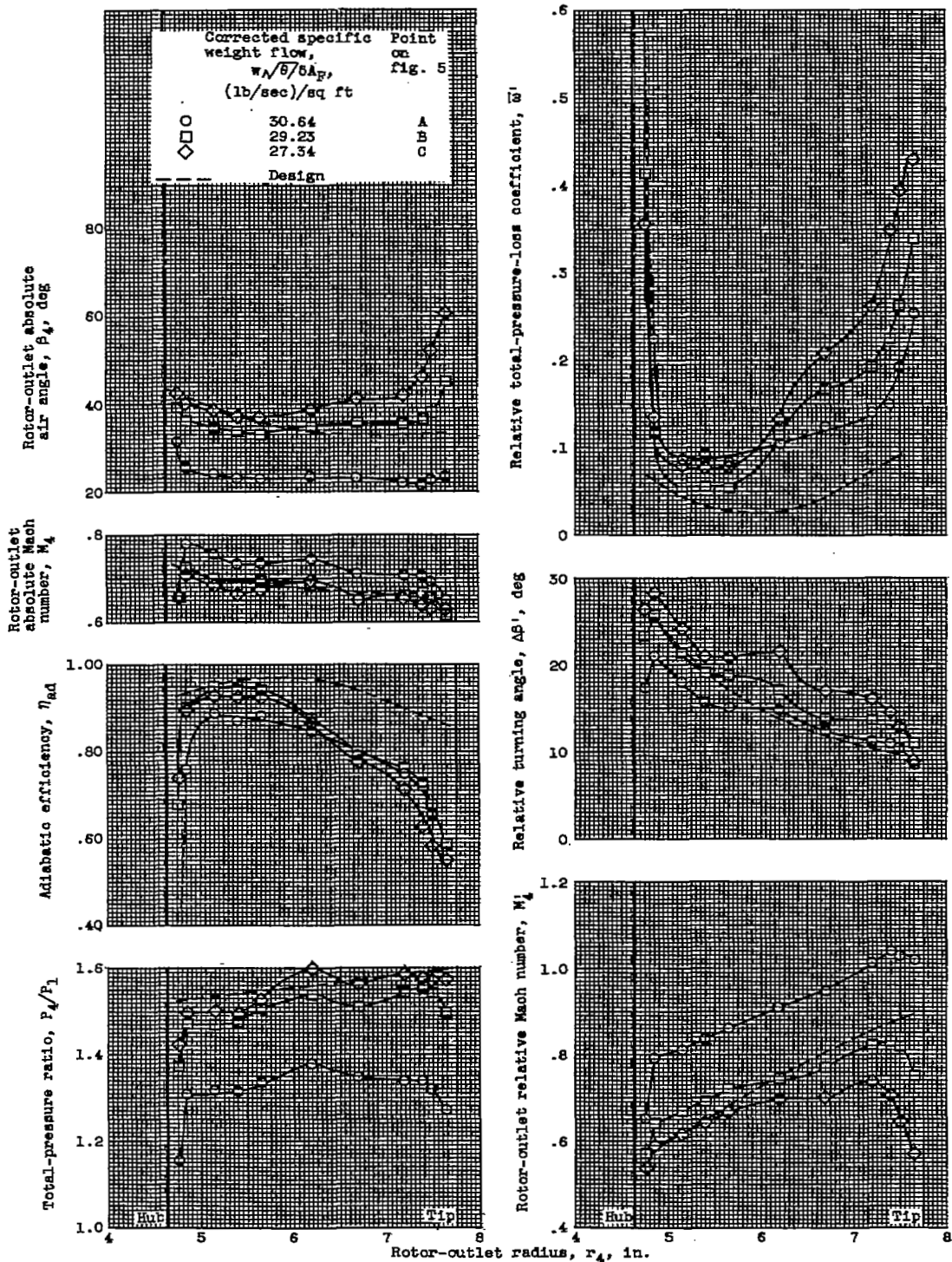
Figure 6. - Continued. Radial variation of rotor-inlet parameters at design speed for three values of corrected specific weight flow.



(c) Relative air angle.

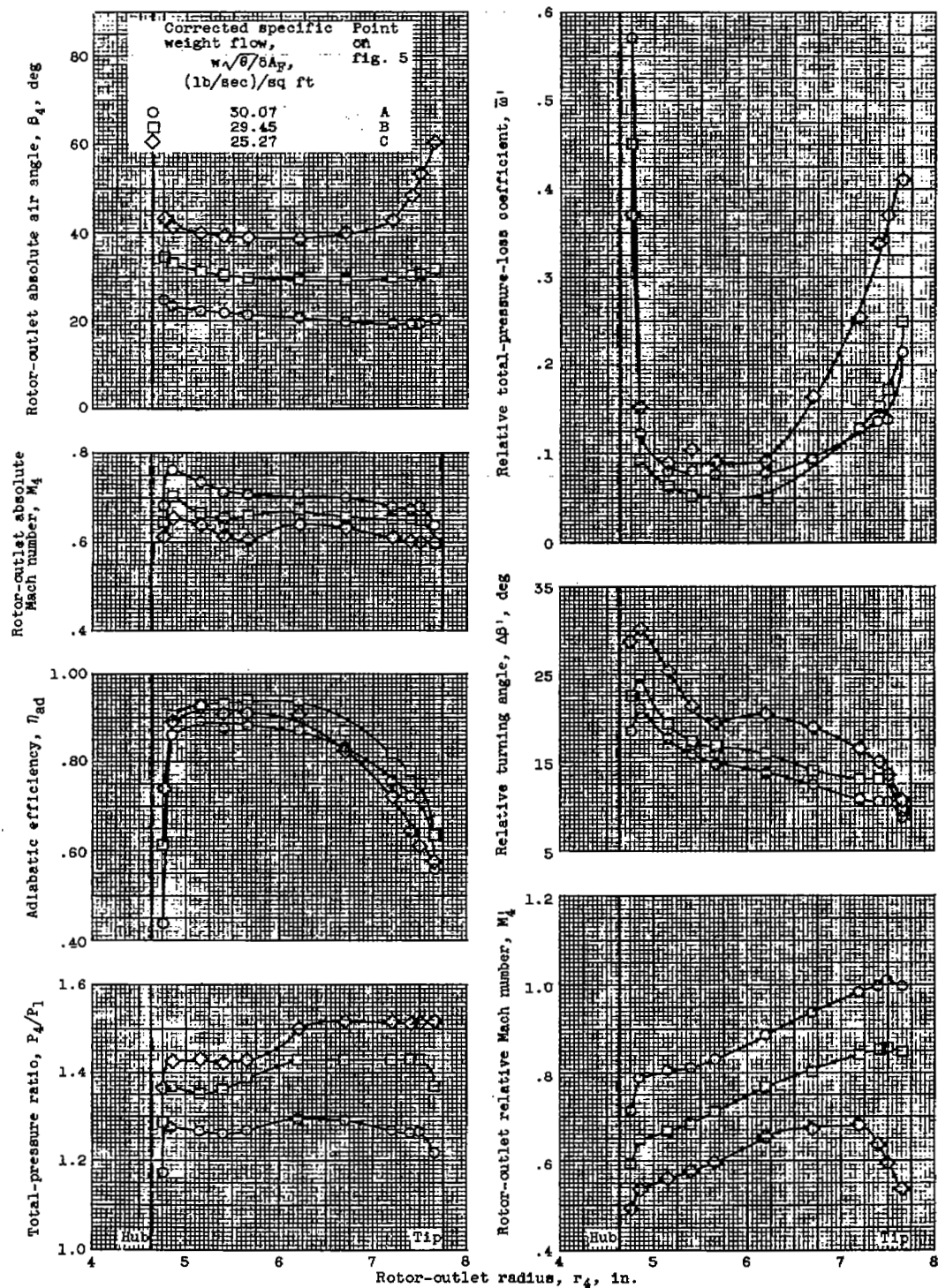
Figure 6. - Concluded. Radial variation of rotor-inlet parameters at design speed for three values of corrected specific weight flow.

4001



(a) Corrected tip speed, 1300 feet per second.

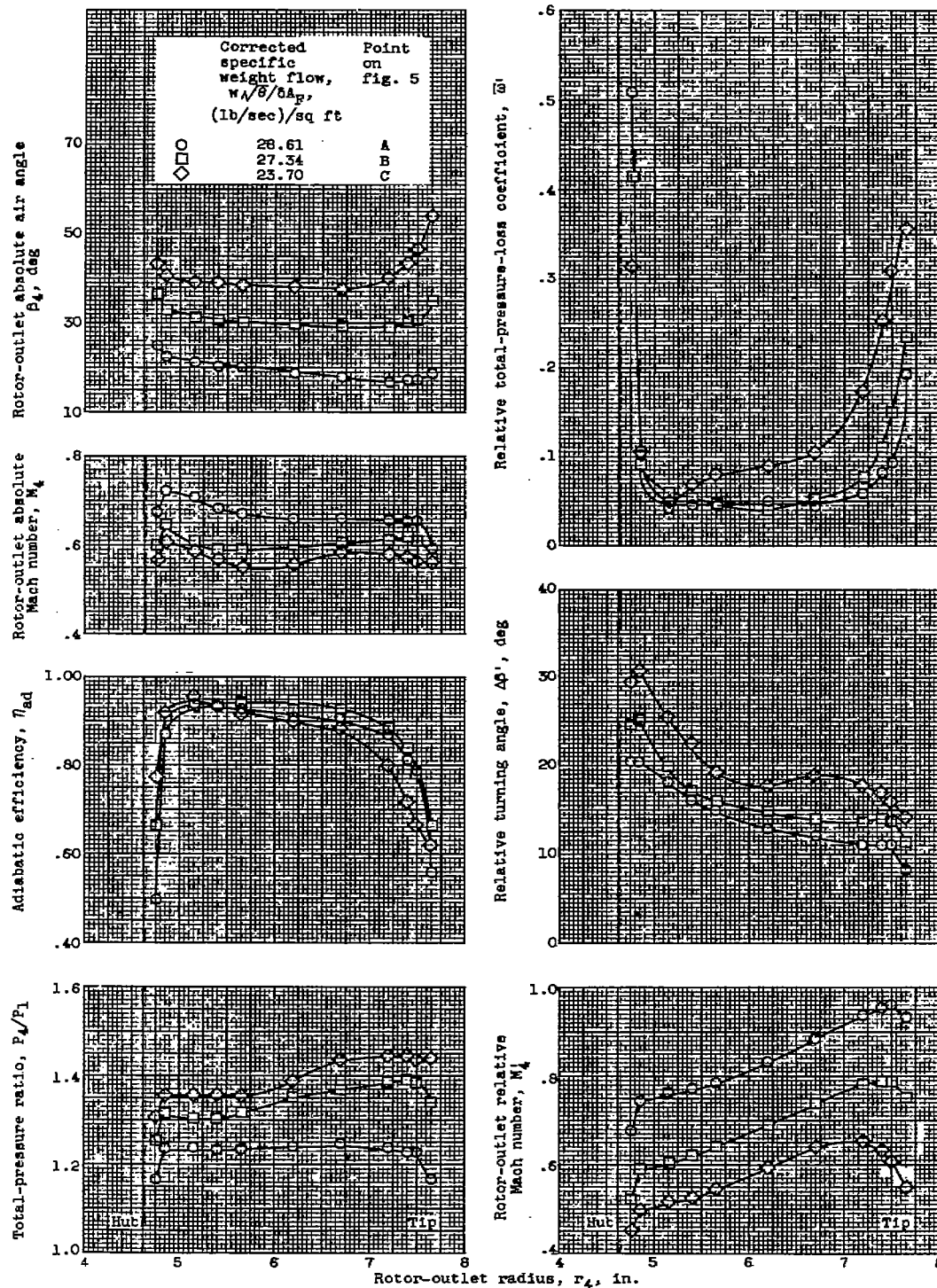
Figure 7. - Radial variation of rotor-outlet parameters for three values of corrected specific weight flow.



(b) Corrected tip speed, 1200 feet per second.

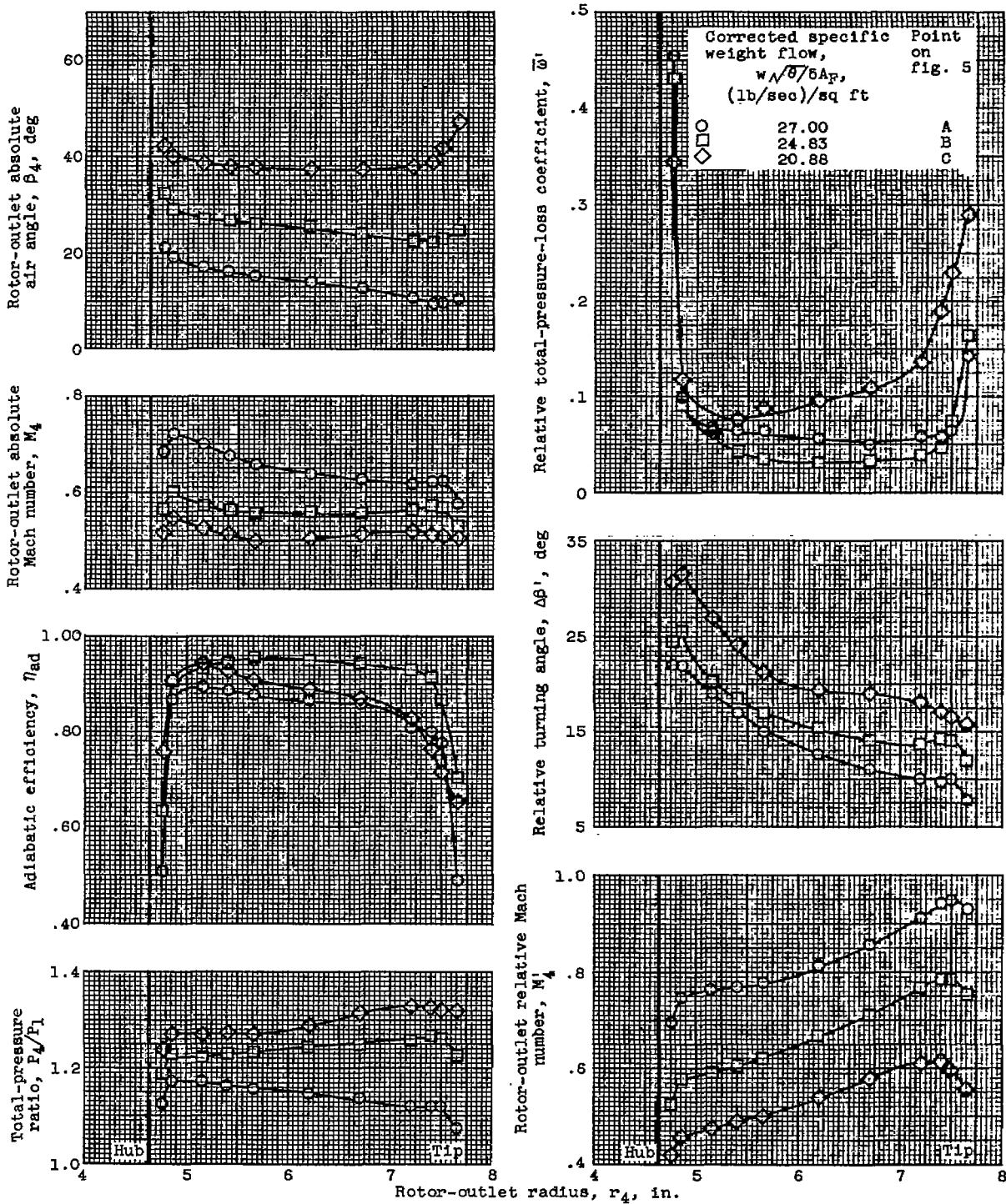
Figure 7. - Continued. Radial variation of rotor-outlet parameters for three values of corrected specific weight flow.

4001



(c) Corrected tip speed, 1100 feet per second.

Figure 7. - Continued. Radial variation of rotor-outlet parameters for three values of corrected specific weight flow.



(d) Corrected tip speed, 975 feet per second.

Figure 7. - Concluded. Radial variation of rotor-outlet parameters for three values of corrected specific weight flow.

CU-7 4001

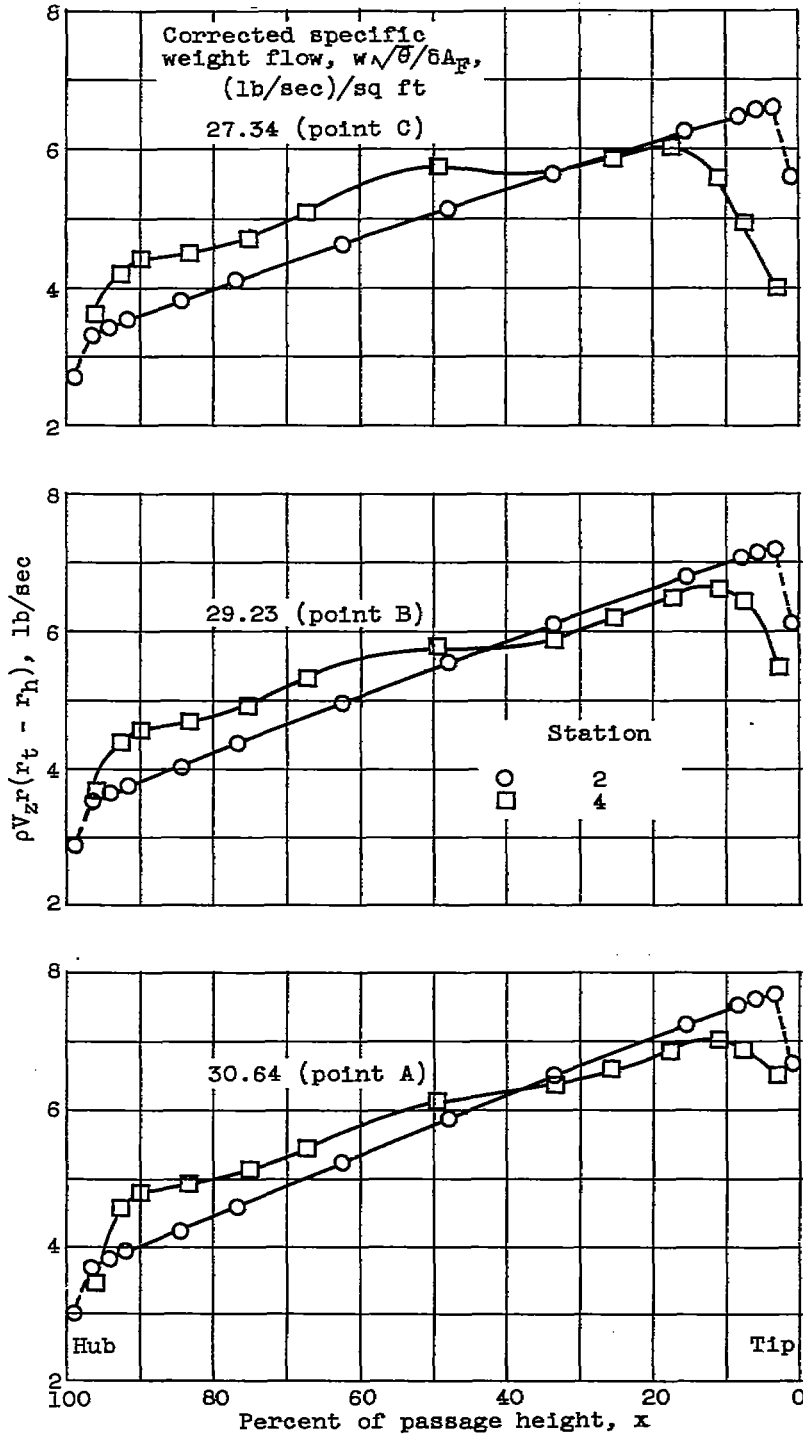
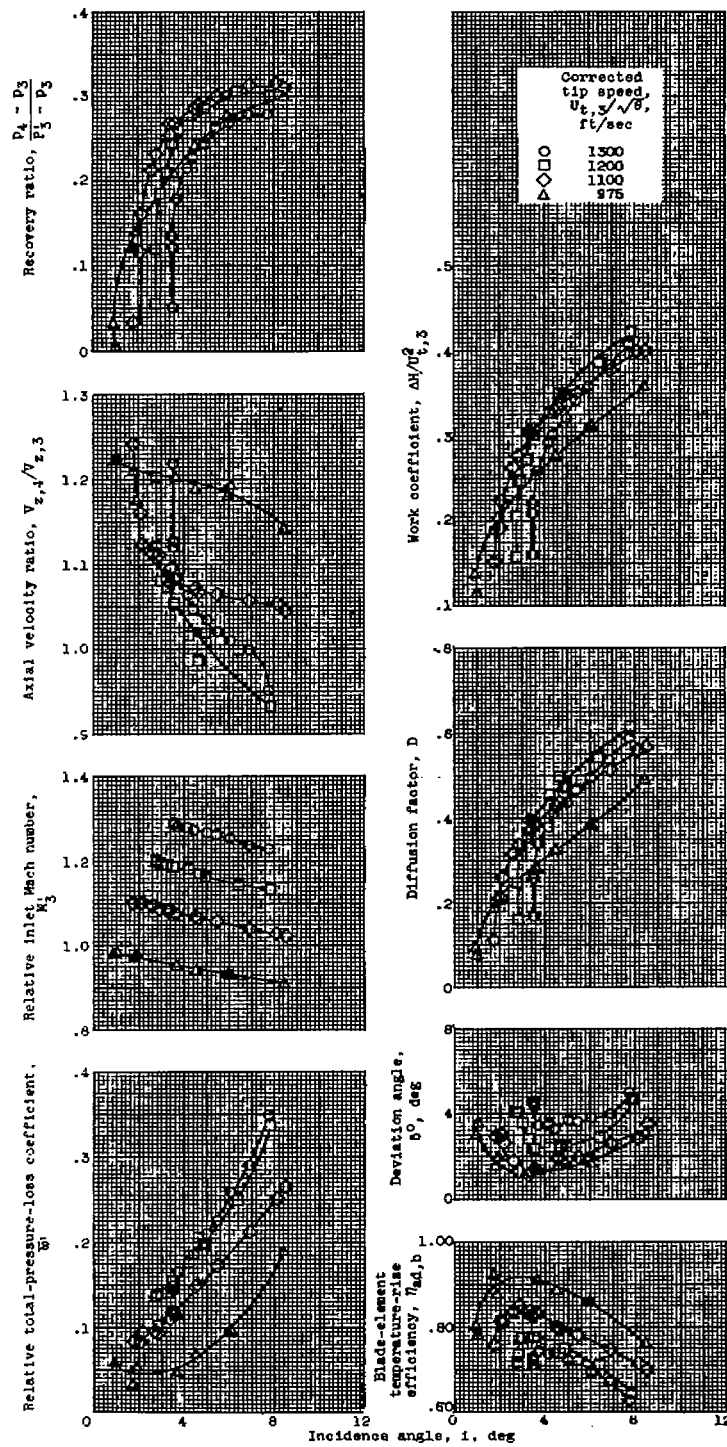


Figure 8. - Radial distribution of weight flow at design speed for three values of corrected specific weight flow.

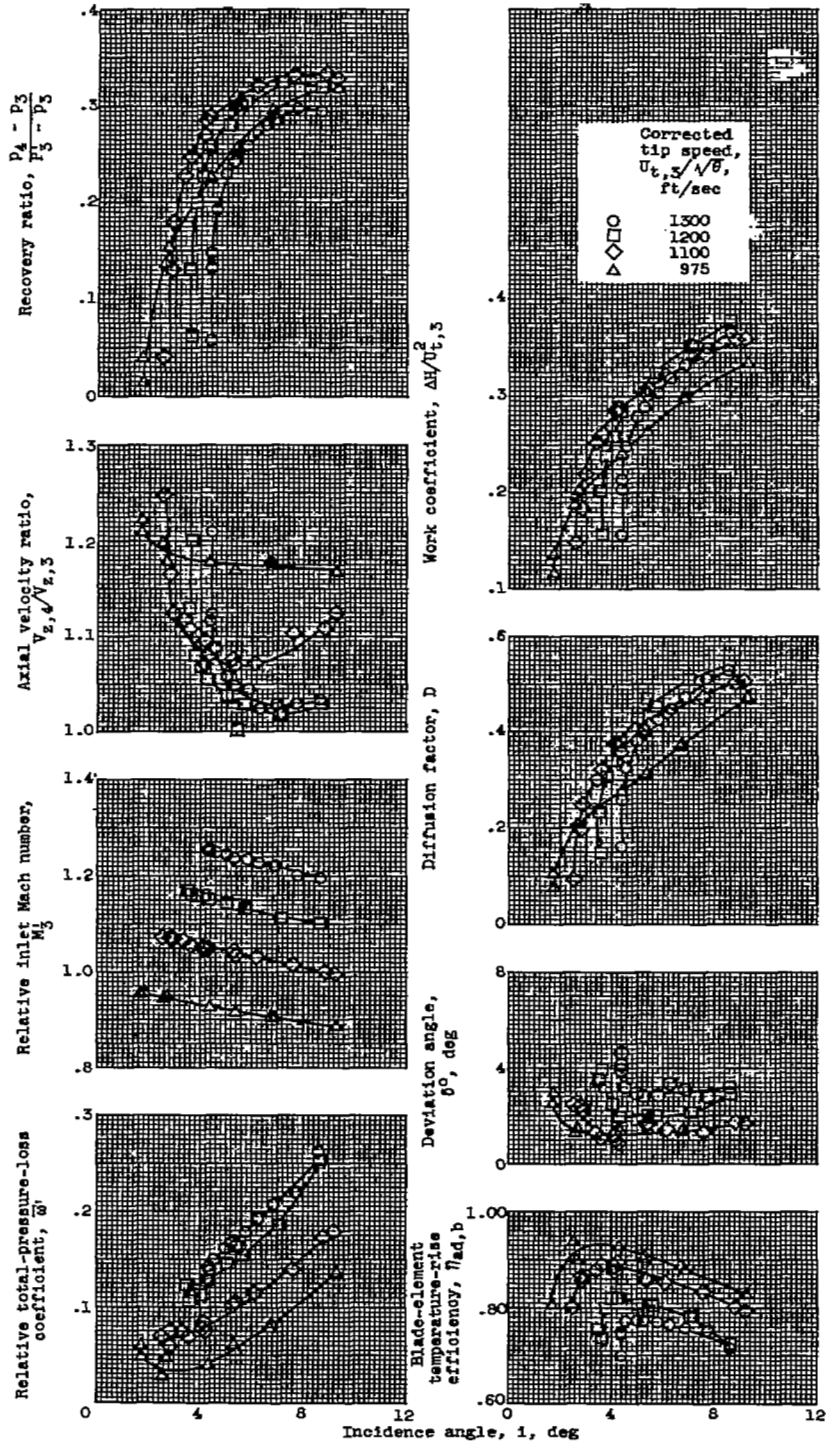


(a) 11 Percent of annulus height. Inlet radius, 7.55 inches; outlet radius, 7.41 inches.

Figure 9. - Blade-element characteristics.

4001

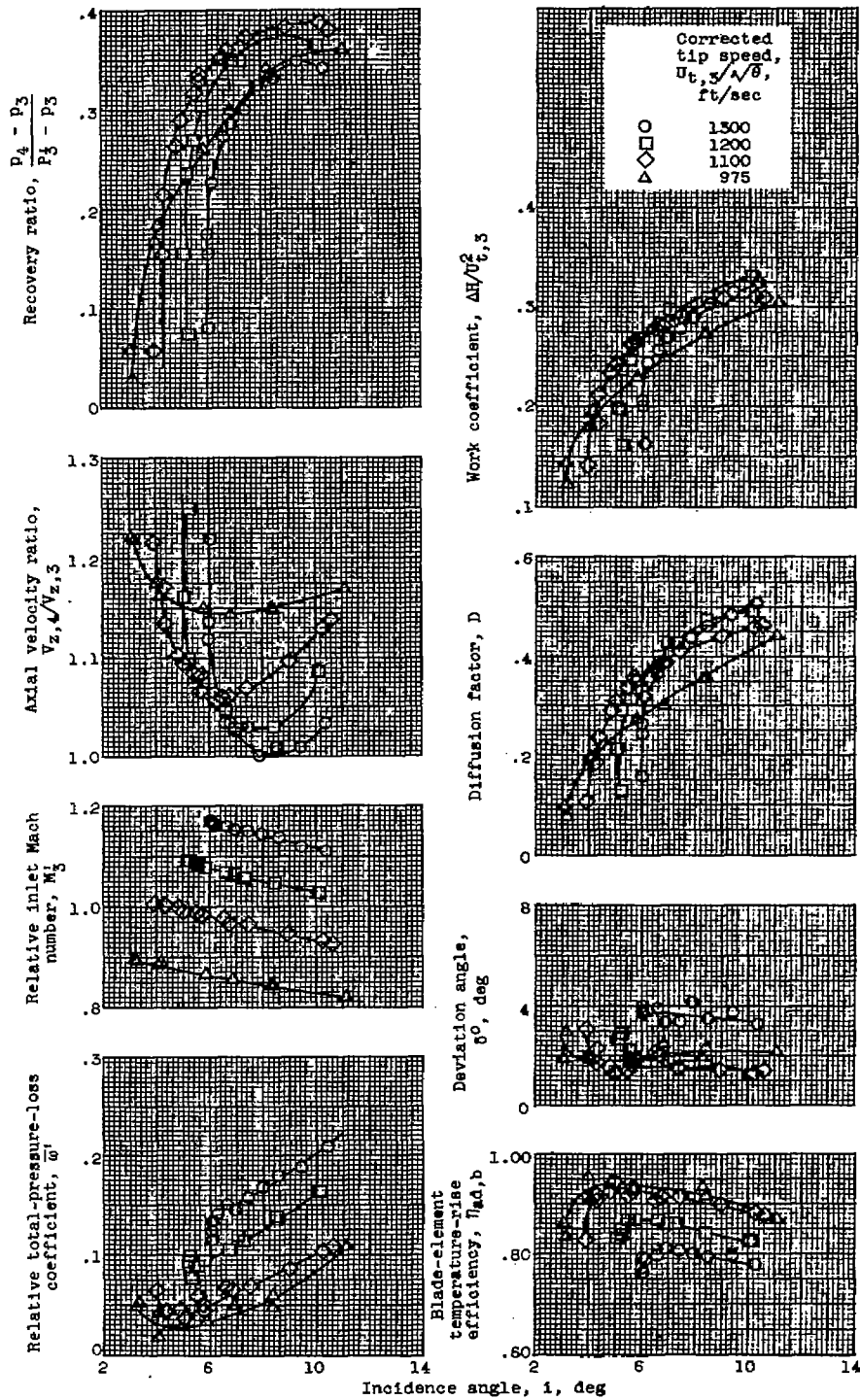
CU-7 back



(b) 17.5 Percent of annulus height. Inlet radius, 7.28 inches; outlet radius, 7.20 inches.

Figure 9. - Continued. Blade-element characteristics.

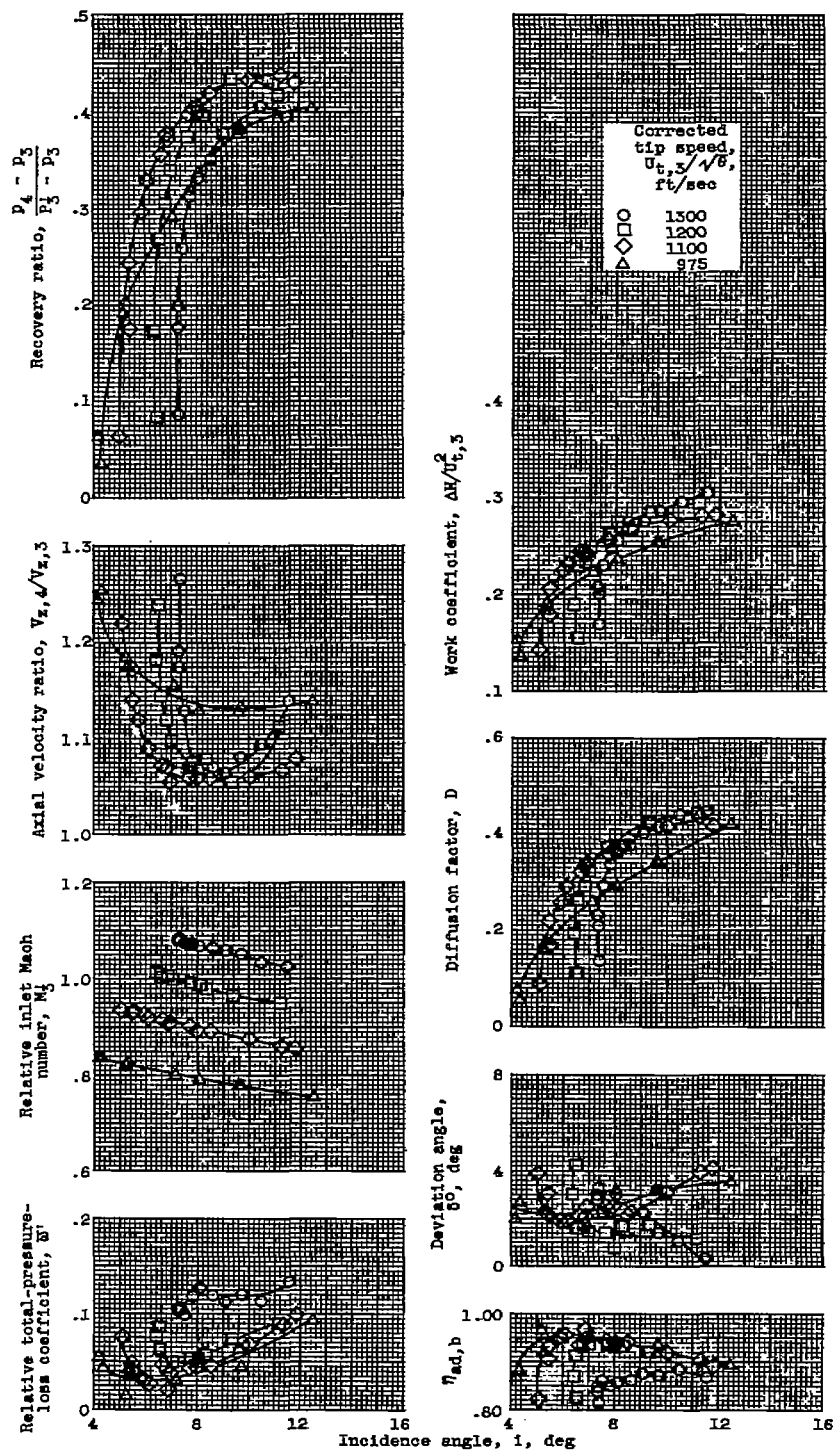
CONFIDENTIAL



(c) 33.5 Percent of annulus height. Inlet radius, 6.64 inches; outlet radius, 6.70 inches.

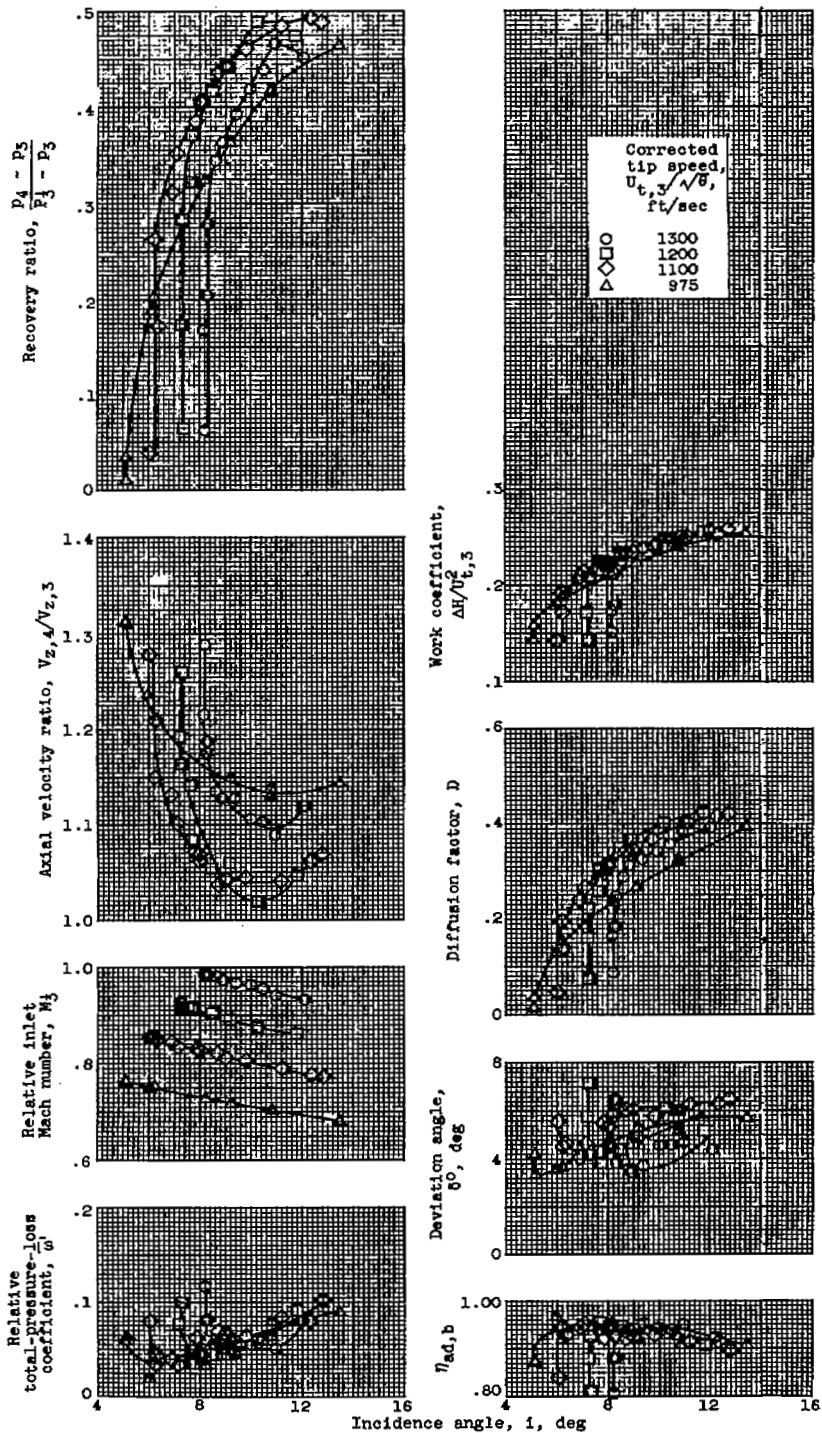
Figure 9. - Continued. Blade-element characteristics.

4001



(d) 50 Percent of annulus height. Inlet radius, 6.00 inches; outlet radius, 5.20 inches.

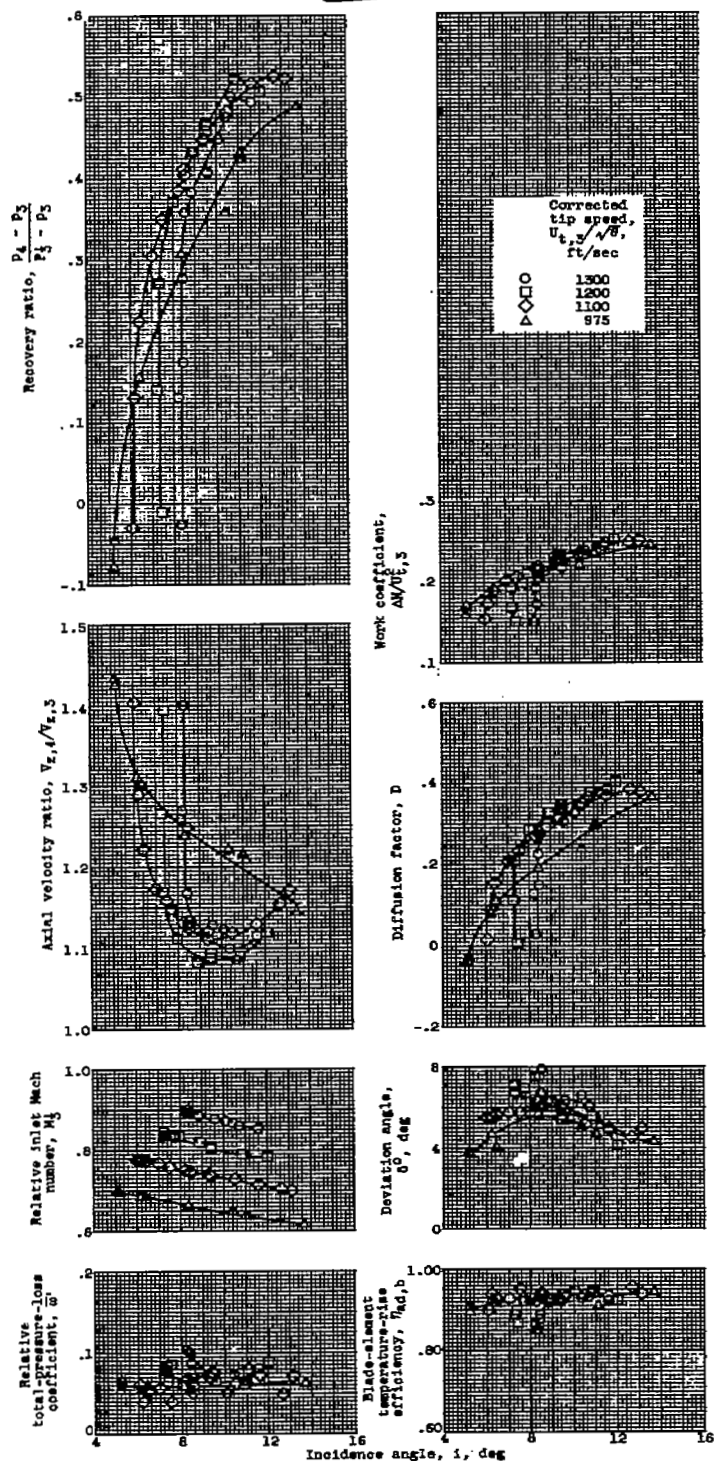
Figure 9. - Continued. Blade-element characteristics.



(e) 67 Percent of annulus height. Inlet radius, 5.28 inches; outlet radius, 5.65 inches.

Figure 9. - Continued. Blade-element characteristics.

4001



(f) 83 Percent of annulus height. Inlet radius, 4.63 inches; outlet radius, 5.16 inches.

Figure 9. - Concluded. Blade-element characteristics.

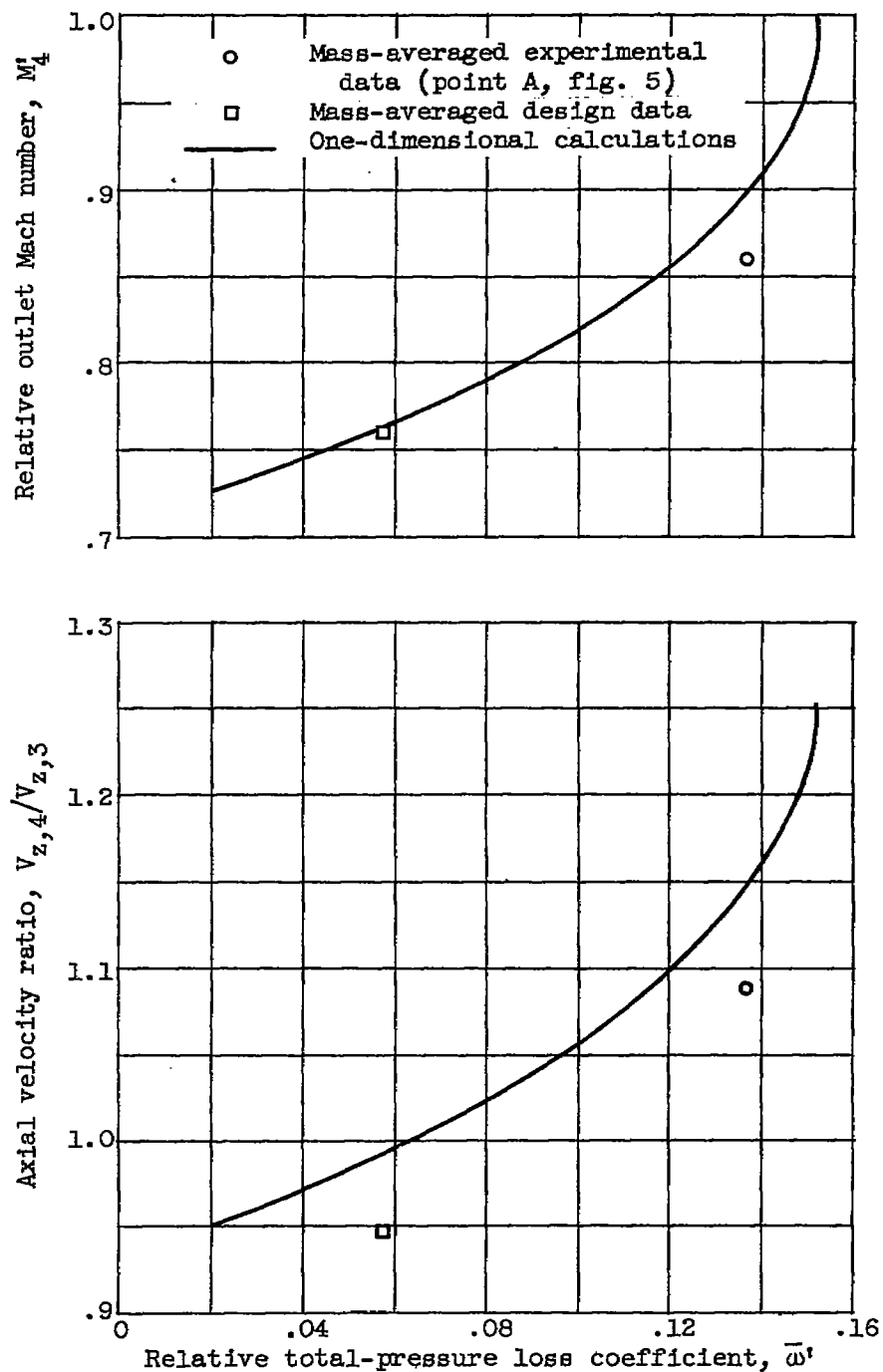


Figure 10. - Calculated one-dimensional variation of axial velocity ratio and relative outlet Mach number with relative total-pressure-loss coefficient.

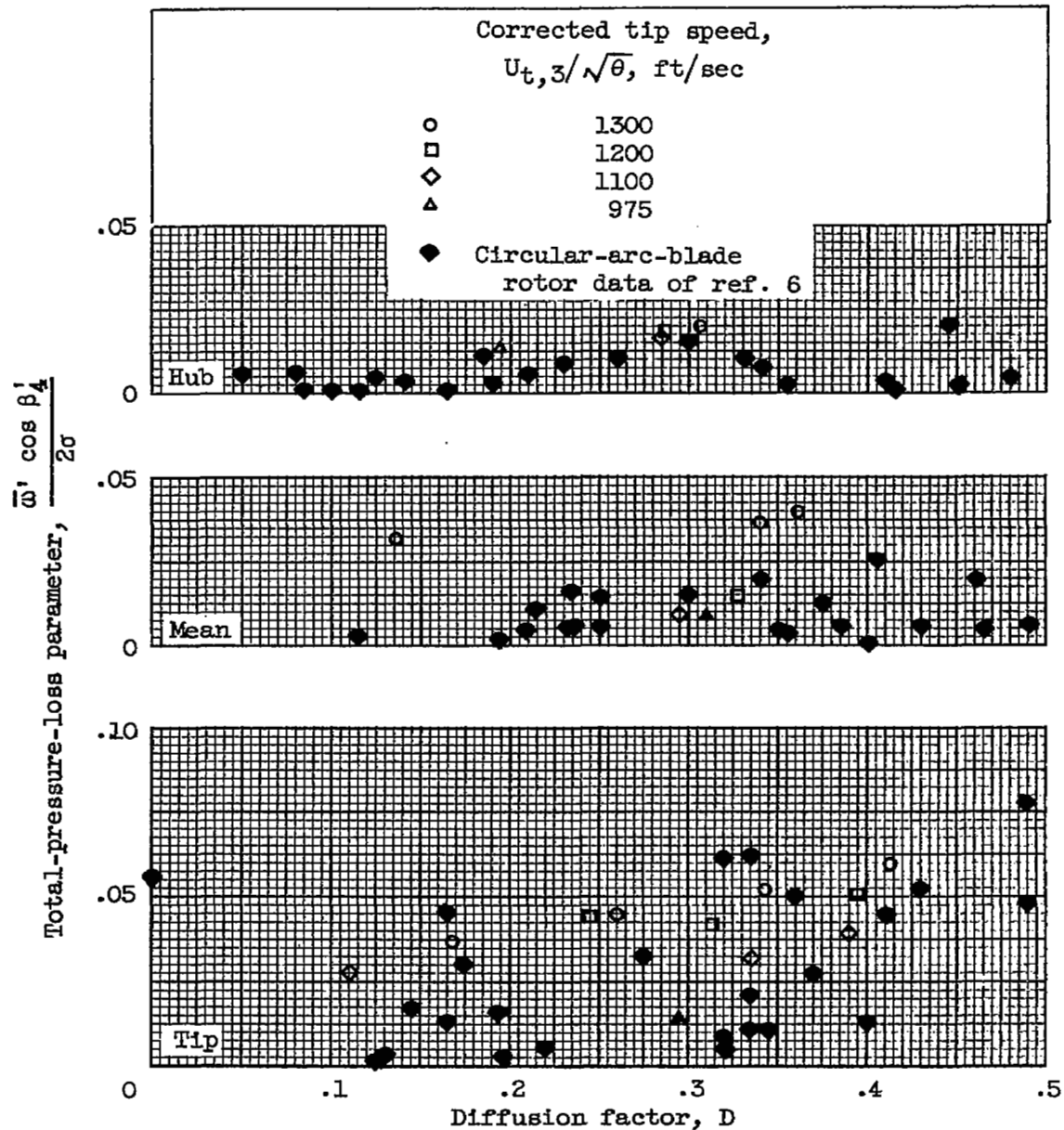


Figure 12. - Variation of total-pressure-loss parameter with diffusion factor at or near minimum-loss incidence angle and comparison with similar data of reference 6.

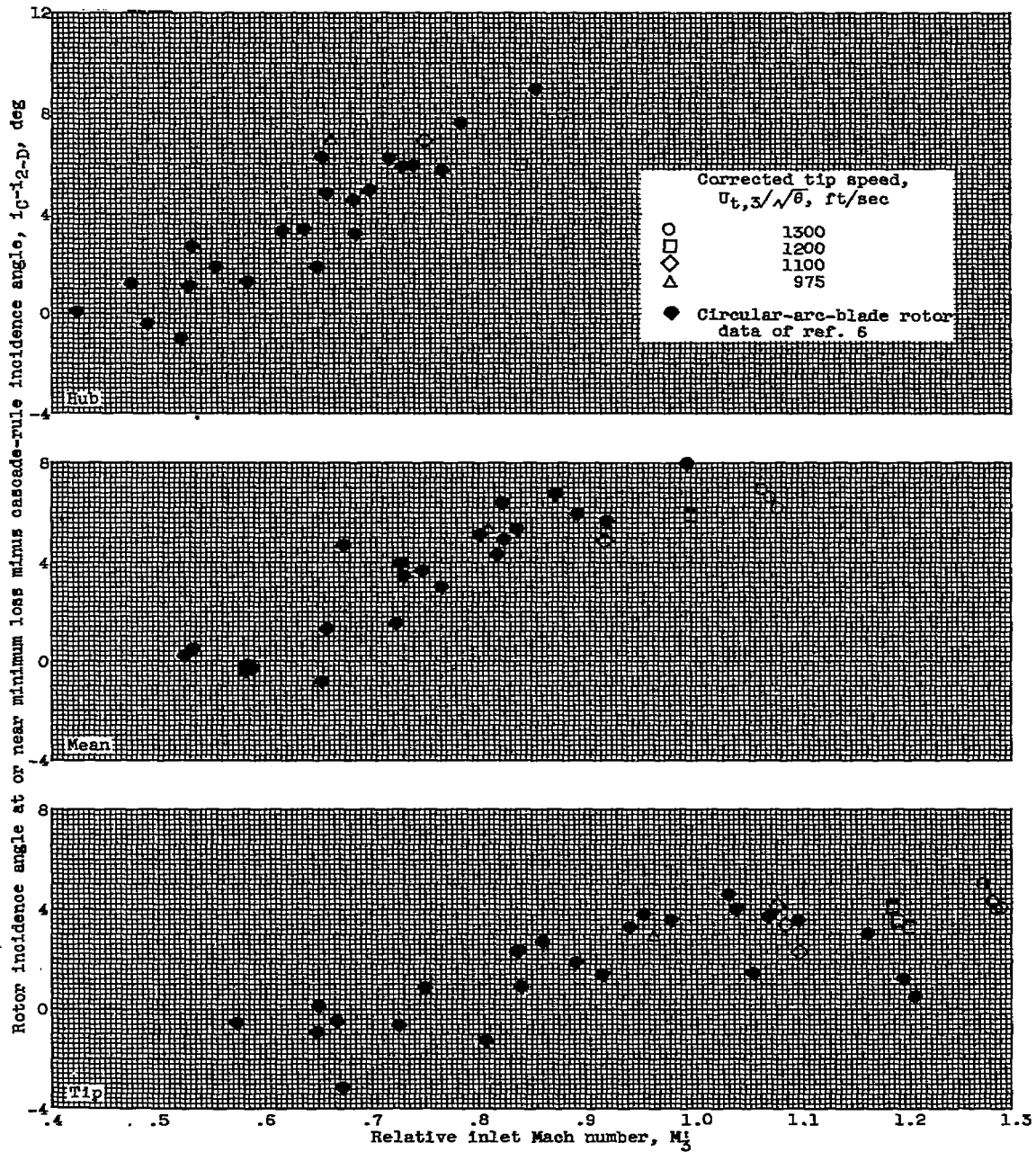


Figure 13. - Variation of rotor incidence angle at or near minimum loss minus cascade-rule incidence angle with relative inlet Mach number and comparison with similar data of reference 6.

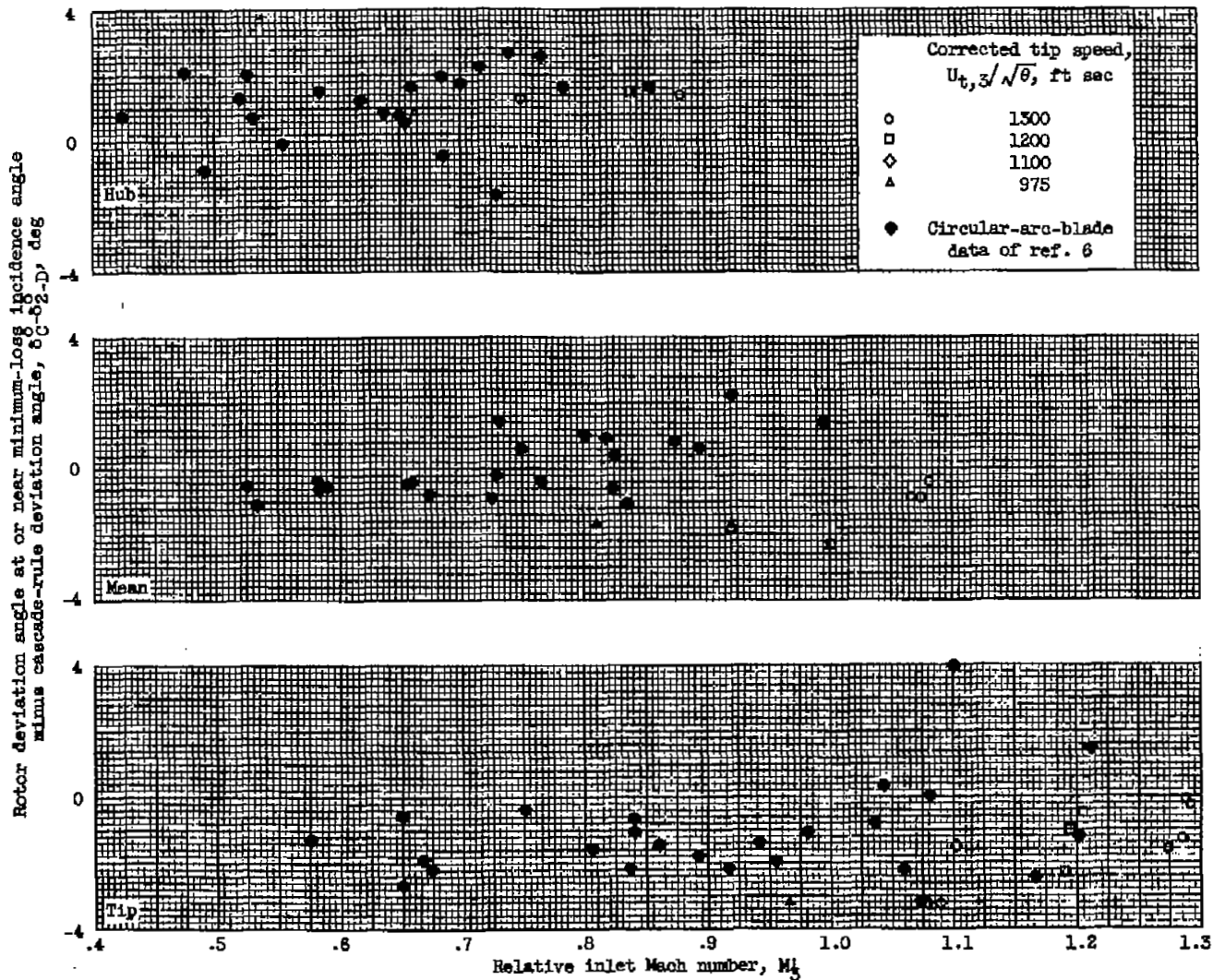


Figure 14. - Variation of rotor deviation angle at or near minimum-loss incidence angle minus cascade-rule deviation angle with relative inlet Mach number and comparison with similar data of reference 6.

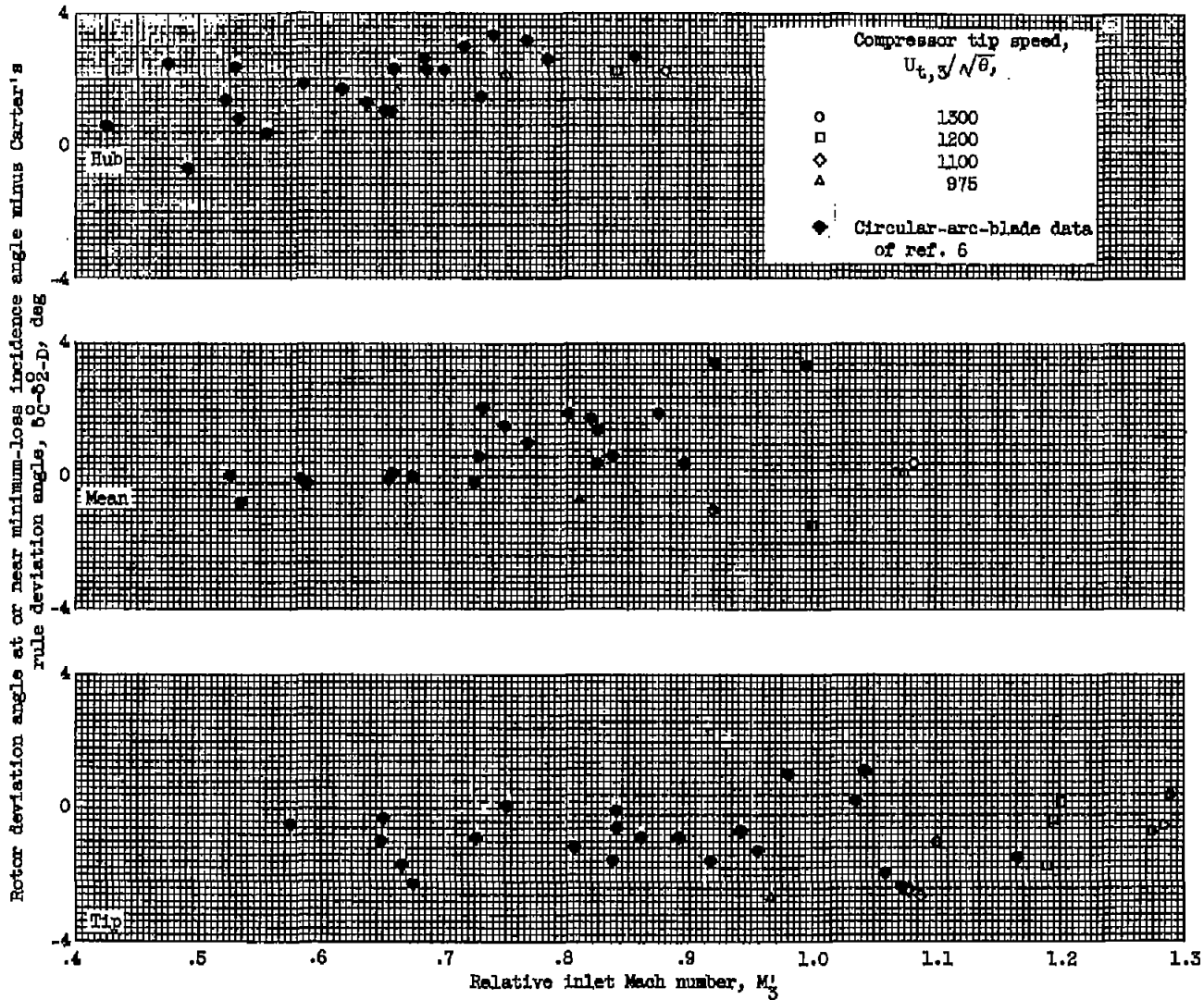


Figure 15. - Variation of rotor deviation angle at or near minimum-loss incidence angle minus Carter's rule deviation angle with relative inlet Mach number and comparison with similar data of reference 6.

[REDACTED]

NASA Technical Library



3 1176 01435 8502



A 1 1 0

C 1 1 1

1
1

1
1

1
1

[REDACTED]